Technical Report ISTC/BES/RS/314

ISTC

ISRO-IISc Space Technology Cell
Indian Institute of Science
Bangalore

Novel techniques to map and monitor forest degradation in the Nilgiri Biosphere Reserve

(Final Technical Report)

R.Sukumar, CES, IISc
Narendran Kodandapani, ANCF,CES, IISc
C.S.Jha, NRSC, ISRO
Sudhakar Reddy, NRSC, ISRO

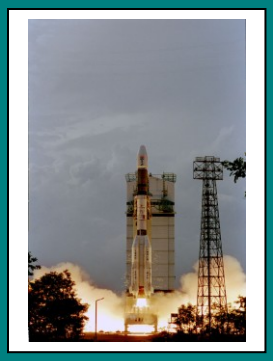

April 2017

Technical Report ISTC/ BES/RS/314

ISRO-IISc Space Technology Cell
Indian Institute of Science
Bangalore

Novel techniques to map and monitor forest degradation in the Nilgiri Biosphere Reserve

(Final Technical Report)

R.Sukumar, CES, IISc
Narendran Kodandapani, ANCF,CES, IISc
C.S.Jha, NRSC, ISRO
Sudhakar Reddy, NRSC, ISRO

April 2017

Project Title: Novel techniques to map and monitor forest degradation in the Nilgiri Biosphere Reserve	Project Code: ISTC/BES/RS/314 Date of Commencement: 01:04:2013 Date of Closure: 31:08:2016
Investigator from Indian Institute of Science: Prof. R. Sukumar Center for Ecological Sciences IISc, Bangalore (rsuku@ces.iisc.ernet.in) Dr. Narendran Kodandapani Senior Scientist, ANCF C/o CES, IISc, Bangalore. Affiliation with email	
Investigator from ISRO Dr. C.S. Jha Group Head Dr. Sudhakar Reddy Scientist SE Forestry and Ecology Group National Remote Sensing Centre (ISRO) Hyderabad 500625, A.P.	
Type of the project: (Research/Development/etc.	
Security classification if any: Open/Restricted	
Short Abstract: The project aims to understand the complex interactions of forests with anthropogenic and climatic factors in the Nilgiri Biosphere Reserve, a biodiversity hotspot. The research involves monitoring, mapping landuse/landcover changes and quantification of forest degradation and drought, using available field and satellite data on vegetation, temperature and precipitation.	
Keywords: Forest change, Classification, Change detection, Degradation , Monitoring Time series , Anomalies	

Total Budget (in lakh) **Rs. 12,37,400**
Products/methodology/algorithms delivered to ISRO/DOS Centre
Where it is put into use/embedded in ISRO/DOS activities/programmes
Number of JRF/students involved (give details of students PhD/MTech) 1. Mr. Beependra Singh. JRF Email Id: beependrasingh@yahoo.com
Number of papers published (International & National Journals/ Conferences etc) Two manuscripts are being prepared.
Patents Not applicable

Acknowledgements

This study was conducted at the Center for Ecological Sciences, Indian Institute of Science, Asian Nature Conservation Foundation (c/o CES, IISc), and Forestry and Ecology Group, National Remote Sensing Centre (NRSC) Hyderabad. We are very grateful to these institutions for providing us research facilities and guidance. We thank ISRO–IISc Space Technology Cell at Indian Institute of Science for funding this project.

We thank the Forest Departments of Karnataka, Tamil Nadu and Kerala for permissions to carry out field work in the project study area. We would like to specially thank the Principal Chief Conservator of Forests (Wildlife) and Chief Wildlife Warden, Tamil Nadu, District Forest Officer, Nilgiris South Division, Field Director, Sathyamangalam Tiger Reserve, Principal Chief Conservator of Forest (Wildlife) and Chief Wildlife Warden, Karnataka, and Conservator of Forest and Field Director of Bandipur Tiger Reserve, Karnataka. The Range Forest Officers of different ranges cooperated with us during the survey; special thanks are due to Mr. Nataraj, Range Forest Officer of Moolehole Range for his extensive help in collecting transect data.

We would like to thank Dr. H.S. Suresh for his help in identification of plants and preparation of herbarium. We gratefully acknowledge the help by Mr. C. M. Bharanaiah, Krishna and other field assistants during the field work and stay at the IISc Field station at Masinagudi, Tamil Nadu.

We thank K. Karthik for introducing us to the use of “R” for spatial analysis and helping us with data processing. We also thank Mr. E. Elango, Scientist, NRSC, ISRO/DOS Balanagar, Hyderabad, for help in procurement of satellite imagery.

Prof. D. Nagesh Kumar, Centre for Earth Sciences (CeAS) and Department of Civil Engineering at IISc provided valuable suggestions, while Prof. C. Jeganathan, Birla Institute of Technology, Ranchi, commented on the use of spatial temporal time series data sets. Several students and staff at CES, IISc, especially Sandeep Pulla, make valuable suggestions on the research methods and reviewed the results.

Lastly, we acknowledge Asian Nature Conservation Foundation for use of their GIS and Remote Sensing conservation database for southern India. This helped us to select a study area extending beyond the Nilgiri Biosphere Reserve to Elephant Ranges 7 and 8.

Abstract

Deforestation is a worldwide problem and has many negative consequences for the natural environment, including changes in ecological processes, biodiversity, biogeochemical cycles and carbon stocks. Satellite-based remote sensing is a cost-effective way to monitor changes in forest cover and degradation over large geographic areas which is not possible by traditional survey methods. This report examines the suitability of different types of satellite data for mapping and monitoring vegetation change and degradation in the Nilgiri Biosphere Reserve (NBR) and adjoining areas in the Western Ghats and Eastern Ghats of southern India. The NBR region features diverse vegetation species across the elevation and rainfall gradient making it a complex system to study vegetation and land use change. The NBR has witnessed major changes in land use and land cover since the mid-19th century, and evaluating these changes, especially in recent decades, is useful for urban planners, policy makers and natural resource managers. We evaluated vegetation cover dynamics of the NBR and the adjoining landscape for the period of 1973 to 2014 using several types of remotely sensed data.

Using thematic maps from remotely-sensed data, the study documented temporal changes in land use and land cover over a period of 38 years captured during 1973 (Landsat 1 MSS), 1992 (Landsat TM) and 2011 (IRS P6 LISS3) for 17 landscape elements that could be distinguished. The area under dry thorn forest, moist deciduous forest, coffee, tea and coconut overall increased. On the other hand, there was reduction in area under agriculture barren land, wet evergreen forest, burned area and grassland/shola forest. The comparative analysis of land use and land cover suggests that there is no visible improvement in forest status.

The nature and extent of forest degradation across the landscape was examined using Spectral Mixture Analysis (SMA) and Change Vector Analysis (CVA) of the above satellite-derived data for 1973, 1992 and 2011. SMA considered the proportions of three endmembers, namely, photosynthetic vegetation, bare soil and shade, for each pixel across the landscape, while CVA used the outputs from SMA to evaluate the magnitude and direction of change in these parameters between two time periods. Between 1973 and 1992 the most visible negative change (reduction in vegetation) was seen in the drier Eastern Ghats region, while between 1992 and 2011 the wetter western hills of the Western Ghats experienced the highest negative change. During the decade of the 1970s, the landscape continued to be exploited for natural resources and land use conversion was common. Since 1980 an effort was made to conserve forests through legal means. This is reflected in an overall increase in biomass in the drier areas of the landscape under deciduous forest cover and given protected area status; however there are good reasons to believe that this increase in biomass was partly due to the expansion of an invasive woody plant *Lantana camara*. The other interesting observation, which also has management implications, is that the wetter western parts of the landscape have overall degraded with loss of biomass. While

some of this could be due to land-use change, the possibility of factors relating to climate change in this transformation cannot be ruled out.

The study also examined the condition of vegetation using Moderate Resolution Imaging Spectroradiometer (MODIS) composite Normalized Difference Vegetation Index (NDVI) and Enhanced Vegetation Index (EVI) time series at 16-day intervals to monitor changes in greenness across the landscape during 2001-14. Across the landscape there seems to be overall greening in drier areas covered with dry deciduous and dry thorn forest. Browning is seen in the moist and evergreen forested regions and human-dominated areas of the landscape. The spatial pattern of greening of the eastern side and browning of the western side overall requires adequate explanation. The results of multiple regression model show that rainfall has a positive effect but temperature tends to have negative effect on the vegetation. Using weather data from a ground station (Kargudi) seems to more strongly and realistically show relationships of temperature and rainfall with NDVI & EVI. The study also showed that the relationship between NDVI & EVI and precipitation becomes stronger with a time-lag effect in the model. In future, a methodology can be developed to test the monthly lag between NDVI and precipitation, as NDVI responds to accumulated moisture, using higher spatial and temporal datasets with ground validation.

The role of climatic variation in determining NDVI/EVI values over time across the landscape was then investigated. Land Surface Temperature (LST) and Rainfall records for the landscape were obtained from MODIS and Climate Hazards Group InfraRed Precipitation (CHIRPS) for the period 2001-14. NDVI and EVI curves were able to differentiate vegetation responses to rainfall. While the NDVI index integrates rainfall, temperature and soil water holding capacity, while EVI ignore soil moisture. NDVI and EVI anomalies show a clear relationship with drought years and the occurrence of fire. The LST and rainfall anomalies are dependent at the time when they occur. While increased vegetation stress in the drier forest types was seen during 2002-03, the stress shifted to the more moist western side after 2006. Prolonged stress was found in two periods i.e. 2002-2004 and 2012-2014 in the vegetation, with LST and rainfall anomalies being the reasons behind this. The magnitude of this stress can be related to drought which is episodic, and global climatic oscillations such as El Niño that negatively influences rainfall and vegetation, and La Niña that influences these positively.

For more realistic and accurate assessment of land use and land cover change in a complex tropical landscape, there must be better integration of remotely-sensed data with ground verification through permanent forest plots and weather stations that capture variables such as biomass, temperature and rainfall at finer resolution. This would help advance the study of ecological changes across large landscapes using remote sensing techniques.

Key words: Deforestation, Monitoring, Time Series, Change Detection, Vegetation, Variability

Contents

CHAPTER IV

Nomenclature/Abbreviations

NBR	Nilgiri Biosphere Reserve
IPCC	Intergovernmental Panel on Climate Change
UNFCC	United Nations Framework Convention on Climate Change (UNFCCC)
MODIS	Moderate Resolution Imaging Spectroradiometer
VI	Vegetation Indices
SOS	Start of Season
UNFCCC	United Nations Framework Convention on Climate Change
REDD	Reduced Deforestation and Degradation
CO_2	Carbon dioxide
O_2	Oxygen
GIS	Geographic Information System
EVI	Enhanced Vegetation Index
NDVI	Normalized Difference Vegetation Index
^0C	Degree Celsius
km²	Square Kilometer
°F	Degree Fahrenheit
km	Kilometer
m	Meter
LPDAAC	Land Processing Distributed Active Archive Center
EOS	Earth Observing System
ETM+	Enhanced Thematic Mapper Plus
ENVI	Environment for Visualizing Images
FCC	False Colour Composite
SD	Standard deviation
%	Percent
MSL	Mean sea Level
LST	Land Surface temperature

List of figures:

List of tables

Chapter 1

Introduction

Linking climate factors and land use change with the dynamics of the world's forests and other natural lands is important in understanding the carbon cycle and predicting carbon sequestration potential of natural vegetation under a changing climate (Kurz et al., 2008). Forests are subject to natural dynamic processes as well as human-induced impacts, whereby they undergo change in their structure, species composition, age-size structure and biomass. At times, forest change may be negative, which means there could be some decrease in forest cover or biomass due to natural and anthropogenic factors, but there can also be positive change from natural factors as well as afforestation, reforestation and management activities.

Several studies show global forest declines in recent decades (Hansen et al., 2013; Riiters et al., 2016; Liang et al., 2016). Change detection is of great interest to economic policy makers, town planners, timber industry, natural resource managers and ecologists tasked with the management of forests (McIver and Wheaton, 2005; Wulder, 1998). A forest is generally defined as a plant community with predominantly woody vegetation. Food and Agriculture Organization (FAO) of United Nations defines forest as land with a tree canopy cover of more than 10 percent and area of more than 0.5 ha (FAO, 2013). Forest is defined by the presence of trees but also by the absence of other land uses. Thus, according to FAO, timber and rubber wood plantations are classified as forests, but fruit orchards and trees planted under agro-forestry systems are categorized as other lands with trees outside forests. Monitoring changes in forested landscapes is important for modeling ecological and environmental processes at local, regional and global scales (Houet et al., 2011). The world's natural forests are experiencing high rates of change over the past century due to direct and indirect exploitation of natural resources.

1.1. Motivation and Objectives

The Asian tropics are witnessing one of the highest rates of deforestation, with consequences for biodiversity in the region (Laurance, 2007). In India, several studies (Menon and Bawa, 1997; Jha et al., 2000) have estimated deforestation rates and forest fragmentation in the Western Ghats (WG); only about 6.8% of the original vegetation of the WG remains (Myers et al., 2000). Recent estimates indicate 0.44% rate of change per year corresponding to about 29 km^2 as the deforestation rate for the WG between 1977 and 1999 (Lo Seen et al., 2010). The bulk of research in the tropics has focused on deforestation or static evaluations of forested areas, seldom have they considered the contributing effects of landscape processes and biotic pressures in the loss of forest cover (Ramesh et al., 1997; Das et al., 2006).

Although they have been studied separately to varying degrees, the combined ecological impacts of forest fragmentation, in unison with biotic pressures such as grazing, logging, and forest fires,

are poorly understood. In recent years many studies have reported an increase in the number of wildfires and the area burnt in different terrestrial ecosystems across the globe (Westerling et al., 2006; Van der Werf et al., 2006; Aragão et al., 2007). Studies in the Western Ghats have revealed a three-fold increase in fire-frequency in the past 100 years (Kodandapani et al., 2004). Similarly, studies have shown a proliferation of invasive species in the Western Ghats (Hiremath and Sundaram, 2005; Ramaswami and Sukumar, 2013). A historical study of the Nilgiri landscape has also shown increased grazing pressures on forests from adjoining human habitations (Prabhakar, 1994). A large area of the Western Ghats has recently been notified as Ecologically Sensitive Zone by the government. It is therefore of interest to quantify the changes in land use and land cover as precisely as possible in this region.

Here, we propose a novel approach to developing a forest degradation map for the Nilgiri Biosphere Reserve (NBR) in the Western Ghats by considering not only the extent of deforestation but also by considering forest degradation due to anthropogenic factors. This could provide insights into patterns of forest degradation in Indian ecosystems while simultaneously giving inputs to estimating carbon dynamics in these ecosystems. Reducing the emissions from deforestation and degradation (REDD) as well as sequestering carbon through forest protection are among the most cost-effective mechanisms for climate change mitigation (Smith and Scherr, 2003; Agrawal et al., 2011).

The Nilgiri Biosphere Reserve (NBR) is spread over the states of Karnataka, Kerala, and Tamil Nadu. The forested area of the reserve is 5520 km^2 (Sukumar, 1990). The NBR supports all major vegetation types of peninsular India (Champion and Seth, 1968). Simultaneously the NBR is under considerable human pressures that impacts a variety of natural resources. Although there are a few estimates of deforestation in the Western Ghats (Jha et al., 2000), there is an urgent need to map, monitor, and assess the extent of forest degradation in the NBR. It must be kept in mind that change in forest ecosystems over decadal time-scales may come about not only through anthropogenic pressures but also climate-induced factors. It is thus important to understand the relative importance of both these factors in vegetation dynamics.

1.1.1. SPECIFIC AIMS/ OBJECTIVES OF THE PROJECT:

The following aims and objectives were mentioned in our project proposal:

1. Create a base current land cover/land use map of the NBR. While some map products do exist for the NBR they are insufficient for the proposed analyses. We propose to generate high-resolution (24m pixel) land cover maps of the NBR using IRS LISS III imagery.

2. Develop spatially explicit maps of forest degradation in the NBR. In order to capitalize upon the extensive spatial dataset of forest fragmentation, fire occurrence, invasive

species, logging, and grazing, we will concentrate analyses of how multiple disturbances interact at the NBR landscape scale. Multi-temporal series of high-resolution satellite data, related to known and detected disturbance events will be analyzed to develop spatially articulated disturbance regime maps.

3. Assess aboveground biomass changes useful for REDD inventories: In recent years reduced emissions due to deforestation and degradation (REDD) have be-come important as a climate change mitigation mechanism (IPCC 2016). We will assess the effectiveness of the methods developed here to assess their use in inventories of REDD+.

4. To assess ecological responses of environmental changes affecting the distribution and dynamics of vegetation with spatio-temporal datasets with spatial statistics and time series analysis.

5. To access the spatial pattern of drought using the spatio-temporal anomalies of vegetation and climatic variation of the landscape.

1.2. Literature survey

Extraction of spectral information from satellite imagery depends on the characteristics of image features such as size, shape, tone, texture, shadow, pattern, and association (Patra, 1977). Spectrally homogenous pixels are grouped together for differentiation. In the literature we found many change detection techniques that have improved over time; these include spectral change identification with pixel-wise operation, raw image differencing, change vector analysis, image ratioing (NDVI, EVI, etc), albedo differencing, vegetation index differencing, hybrid methods, multi-date principal component analysis and post-classification technique. Change detection is the most commonly used technique in various applications such as land use and land cover changes, habitat fragmentation, rate of deforestation, coastal change, urban sprawl, and also in spatial and temporal analysis with GIS (Geographic Information System) and Remote Sensing with digital image processing techniques (Ramachandra et al., 2004).

To assess changes in land cover, satellite imagery from similar time periods are used to minimize the variability in vegetation phenology. Spectral properties are different due to angle of the sun, and phenological inconsistencies arise because of local precipitation and temperature variations which result in problems in differentiating real change in land cover from changes in spectral properties due to seasonal effects (Coppin et al., 2004). The accuracy of change detection depends on spectral, spatial, and temporal characteristics of the multi-date imagery, precise registration, calibration, and normalization between multi-temporal images especially in complex landscapes. Change detection techniques using the analyst's experience, familiarity with the study area and the availability of quality ground reference data for accuracy assessment, is time

consuming, restricted and expensive. Researchers have now started using time series and NDVI (Normalized Difference Vegetation Index) curves for understanding trend of vegetation growth, seasonal cycles and land cover classification at global scale (Enkhzaya and Tateishi, 2011; Vuolo et al., 2011).

Moderate Resolution Imaging Spectroradiometer (MODIS) VI products are designed to provide consistent spatial and temporal comparisons of global vegetation conditions that can be used to monitor photosynthetic activity (Huete et al., 2002). Forest change normally does not take place overnight and this is the same with regeneration of forest. Forest change depends on the magnitude of change versus the signal-to-noise ratio often determined by the spectral, spatial and temporal characteristics of the remotely-sensed data (Verbesselt et al., 2010).

In recent years, NDVI datasets from different satellites have been used in assessing vegetation vigor (greenness – changes in green cover), monitoring and detecting changes associated with human activities, ecological changes, climatic variability, and land use and land cover changes (Paruelo et al., 2001). NDVI is related to Photosynthetically Active Radiation (PAR) and primary production of the vegetation cover, density and condition (Herrmann et al., 2005). NDVI has been used to study a variety of biomes from arid zones (Olssaon et al., 2005) to mountain regions globally (Krishnaswamy et al., 2014). A similar index EVI (Enhanced Vegetation Index) has been developed; this is more reliable in measuring the biophysical properties of vegetation, free from atmospheric influences and saturation problems of NDVI at high biomass areas (Huete et al., 2002; Rocha and Shaver, 2009; Setiawan et al., 2013).

1.3. Scope of the project

The Nilgiri Biosphere Reserve (NBR) region has diverse vegetation and land use patterns across an elevation and rainfall gradient where change detection techniques were tested to obtain information on forest degradation. Different classification methods were applied to satellite data available since 1973 from sources such as Landsat MSS, Landsat TM, and IRS LISS3. Historical records show that land has being converted to commercial plantations such as tea, coffee, teak and rubber from the early 1890s (Prabhakar, 1994). We used linear spectral unmixing and change vector analysis techniques to assess the spatial and temporal patterns of changes. These techniques were used to detect areas which have experienced changes in terms of increases in vegetation canopy (biomass increase) or forest regeneration. These techniques are also capable of detecting areas with decline in vegetation and increase in soil fraction because of reduced tree cover.

The availability of MODIS time series data since 2000 at a resolution of 1km can be used to understand the dynamic nature of the landscape. The time series of NDVI and EVI indices which are commonly used for vegetation studies can help us to understand patterns of change and their

possible causes such as climatic anomalies. Studies have reported greening might be due to increase in concentrations of carbon dioxide in the atmosphere that fertilizes the growth of woody plants, including invasive species, in preferences to tropical grasses (Duke and Mooney, 1999; Ramaswamy and Sukumar, 2013). From this project, information regarding the status of forest, land use and land cover changes can help identify areas experiencing degradation which require attention from forest managers for conservation and management.

Chapter 2

Land Cover/Land Use Mapping of the Nilgiri Biosphere Reserve (NBR)

2.1. Introduction

Understanding the pattern of changes in a forested landscape helps to model ecological and environmental processes at local, regional and global scales (Houet et al., 2010; Yang et al. 2012). In addition, forest is an important component of an ecosystem and any major disturbance to this has implications for patterns of regional/global climate. Studies on forest degradation are of great interest and provide vital input to forest managers, planners, timber industry, and ecologists (Wulder et al., 1998; McIver and Wheaton, 2005). There are many ways of extracting information from satellite data such as visual analysis, digital-based visualization, shape and texture, change detection, multispectral classification and multi-temporal dynamics method (Franklin, 2001; Gillanders et al., 2008).

The relationship between land use and land cover is the best available process to understand how people interact with the environment. Understanding land use change is a complex undertaking (Haines, 2009). On a global scale, in the past 20 years land use has experienced extremely rapid change in the Asian dry lands, the Amazon, Southeast Asia, Siberia and Eastern China due to agricultural and urban expansion (Lapers et al., 2005). Land cover has major implications for biodiversity and ecological systems (Hains, 2009). A better understanding of the relationships between land use and land cover can help in future planning and conservation. (Chen et al., 2006). Land use and land cover are key for the future of ecosystem services and biodiversity (Lo Seen et al. 2010; Schroter et al., 2005).

A number of studies have used models for understanding and predicting future trends of land use and land cover arising from increased variability of climatic factors by 2050 (Al-Bakri et al., 2013). Thus, land use changes and transformation are key factor to determining biodiversity and forest cover at different scales (Haines, 2009). It is widely accepted that land use and land cover do not mean the same thing (Jasen et al., 2002). Land cover refers to what is present on the physical surface, and land use refers to social and economic activities performed on this surface. In recent times, interdisciplinary studies have tried to understand the relationships between land use and land cover (Rindfuss et al., 2008). With continuous development in space technology, satellites are providing information with high temporal and spatial resolution. Different change detection techniques are also being developed to study changes in land use and land cover (Singh, 1989; Al-doski et al., 2013; Pathak, 2014).

Spatio-temporal change detection process involves determining land use and land cover transformation from multi-temporal remote sensing data. The aim of this study is to use multi-

temporal data available from Landsat and IRS over a 38-year period (1973-2011) to create current land cover/land use map of the Nilgiri Biosphere Reserve (NBR) and to determine changes in this landscape over this 4-decadel period.

2.2. Materials and Methods

2.2.1. The study area

The study area is a heterogeneous landscape located in the southern Western Ghats and adjoining areas of the Eastern Ghats of peninsular India (**Figure 2.1:**)(Mohandass and Davidar, 2009). It covers an area of 15130 km^2, representing all the major forest types found in the peninsula (Champion and Seth, 1968). The study area falls within the three states of Karnataka (5479 km^2), Tamil Nadu (5665 km^2) and Kerala (3986 km^2). The Nilgiri Biosphere Reserve (5520 km^2) is the first biosphere reserve established in 1986 by the Government of India and later registered with UNESCO (Sukumar, 1990). The elevation of Nilgiri Biosphere Reserve ranges from near sea level up to 2600 m above MSL and follows a west-east topographic and climatic gradient which gives rise to a large diversity in its vegetation types. The mean temperature in the NBR varies with 26^0C below 500m of elevation, around 23^0C between 500-1000m of elevation and below 20^0C above 1000m of elevation.

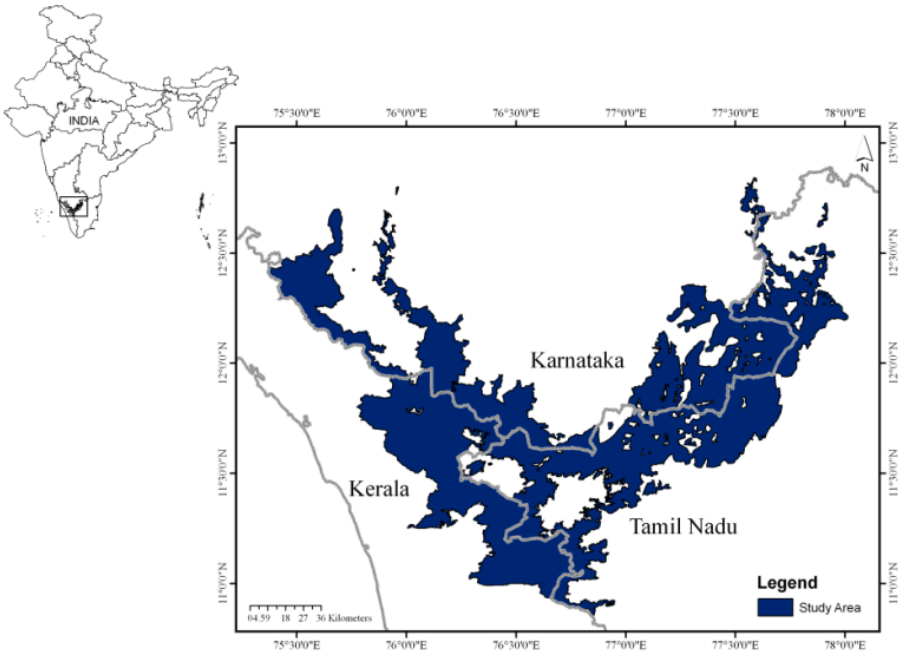

Figure 2.1: Location map of the study area

In some places of the rain shadow areas the temperature in summer (May) goes up to 40^0C while at the highest elevations it dips below freezing point during winter (December-January). The

western side of the NBR receives annual rainfall of about 3000 mm while the sheltered Moyar river valley receives only 400 mm. The study area comprises protected areas (National Parks, Wildlife Sanctuaries and Tiger Reserves) and other territorial forest divisions under the control of the state forest departments, as well as private forests, plantations (chiefly tea and coffee), agricultural land and settlements (Kodandapani et al., 2001). The construction of Hydel and irrigation dams at various elevations has also created large, perennial water bodies.

2.2.2. Data processing:

The data used for studying the historical changes in the landscape include satellite images for Landsat 1 MSS and TM (downloaded from http://glovis.usgs.gov) while IRS data was procured from NRSC, Hyderabad. To minimize the seasonal effect of the images acquired from multiple dates, images of the same time period were chosen for comparing trends over the years. The IRS P6 LISS III satellite was geo-rectified using ancillary data from 1:250,000 Survey of India (SoI) topographic maps. The DNs (Digital Numbers) were converted to radiances and subsequently to TOA (top of atmospheric) reflectance (Hall et al., 1991, Lu et al., 2001).

Table 2.2: Details of satellite data used for the study

Sl.no.	Satellite Sensor	Date of acquisition	Path/row	Spatial Resolution (m)
1	Landsat 1 MSS	10-Feb-1973	155/52	57
2	Landsat 1 MSS	10-Feb-1973	155/51	57
3	Landsat 1 MSS	1-Mar-1973	156/51	57
4	Landsat 1 MSS	27-Feb-1973	154/51	57
5	Landsat 1 MSS	27-Feb-1973	154/52	57
6	Landsat TM	14-Jan-1992	144/51	28
7	Landsat TM	14-Jan-1992	144/52	28
8	Landsat TM	2-Jan-1991	145/51	28
9	Landsat TM	15-Jan-1990	145/51	28
10	Landsat TM	11-Mar-1992	143/52	28
11	Landsat TM	7-Mar-1991	145/51	28
12	IRS P6 LISS III	1-Feb-2011	099/65	24
13	IRS P6 LISS III	10-Mar-2012	098/64	24
14	IRS P6 LISS III	1-Mar-2011	100/064	24
15	IRS P6 LISS III	1-Mar-2011	100/065	24

A methodology was developed specific to the study area is shown in Figure 2.2. Details of different satellite scenes with path/row used for the study are provided in Table 2.1. For all the images the root mean square (rms) error was <0.50 pixel and were geo-registered with the

rectified scene (IRS P6). Finally, all the images were mosaiced to produced three images for the years 1973, 1992 and 2011. The study area was extracted using the boundary of Project Elephant Reserves 7 and 8 of southern India.

2.2.3. Classification

A post-classification change detection technique was used for comparison between the different dates of satellite images. The use of imagery which are different in date and time increases the uncertainty in the classification results. It is a more difficult task to get accuracy assessment of multi-images than for a single image classification (Congalton & Green, 1999). Classification of remote sensing data into numbers of land use and land cover classes depends on the objectives and requirements of the study (Anderson et al., 1976). The classes were decided with reference to a previous map prepared for the entire Western Ghats (Sankar, 2011). Similar classes were used in our study (Table 2.2).

Table 2.2: Land-uses and land-cover classes used for the study

Sl. No.	Classes	Land-uses and land-covers included in a class
1	Agriculture	**Cropland, orchards, vineyards, and nurseries**
2	Barren Land	**Bare exposed rock, quarries and disturbed ground**
3	Burned Area	**Areas experiencing fires**
4	Cloud	**White regions**
5	Coconut/banana	**Commercial plantation**
6	Coffee	**Commercial plantation**
7	Dry Evergreen	**Forest type**
8	Dry Deciduous	**Forest type**
9	Dry Thorn	**Forest type**
10	Grassland	**Shola Grassland & Grasslands**
11	Moist Deciduous	**Forest type**
12	Plantation	**Teak, rubber**
13	Settlement	**Urban settlement**
14	Shadow	**Dark regions**
15	Tea	**Commercial plantation**
16	Water Bodies	**Rivers, lakes and ponds**
17	Wet evergreen	**Evergreen and Semi evergreen**

A total of 423 training sample points were collected from the field as the success of the classification process depends on the accuracy of the training sample points. Prior knowledge is needed in order to classify and characterize the different homogenous classes. Supervised classification with maximum likelihood classification (MLC) technique was adopted to classify each pixel (Foody, 2002). A visual interpretation technique which helps to investigate the variation in the FCC (False Colour Composite) images was employed for the classification and delineation of different spectral classes from the scenes (Dutta et al., 2016). These classes were then clustered to independently determine their identity.

2.2.4. Accuracy assessment:

Accuracy assessment was carried out to test the spectrally-classified inaccuracies by a set of ground truth data. These test samples were then used to create an error matrix (also referred to as confusion matrix), kappa (κ) statistics, and producer's and user's accuracies to assess the accuracy of the classification (Foody, 2002). With the help of GPS, ground verification was done for doubtful cases. Based on the ground truthing the misclassified areas were corrected using recode option in ERDAS Imagine 9.3. A stratified random sampling method was used to generate 900 reference points. These reference points were ground-truthed with the help of Google Earth. All the training sample points along with the reference points were used for accuracy assessment. A statistically valid sampling strategy was adopted to assess commission, omission and overall accuracy of the final classification results. Finally, the contingency table was tested using Kappa statistics (Lillesand and Kiefer, 1999).

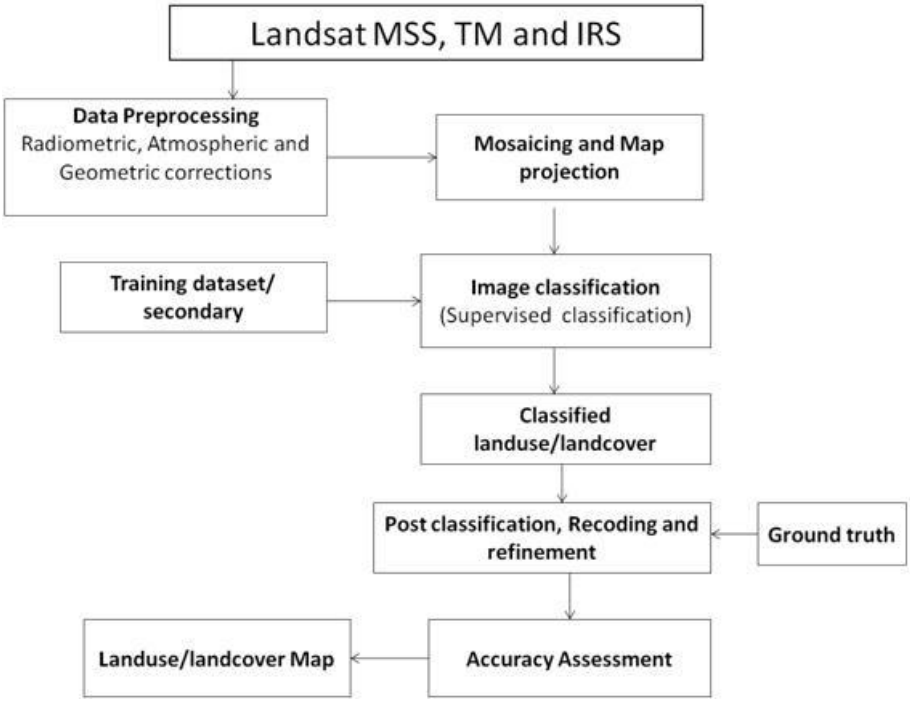

Figure 2.2: Flow chart showing methodology adopted for the study

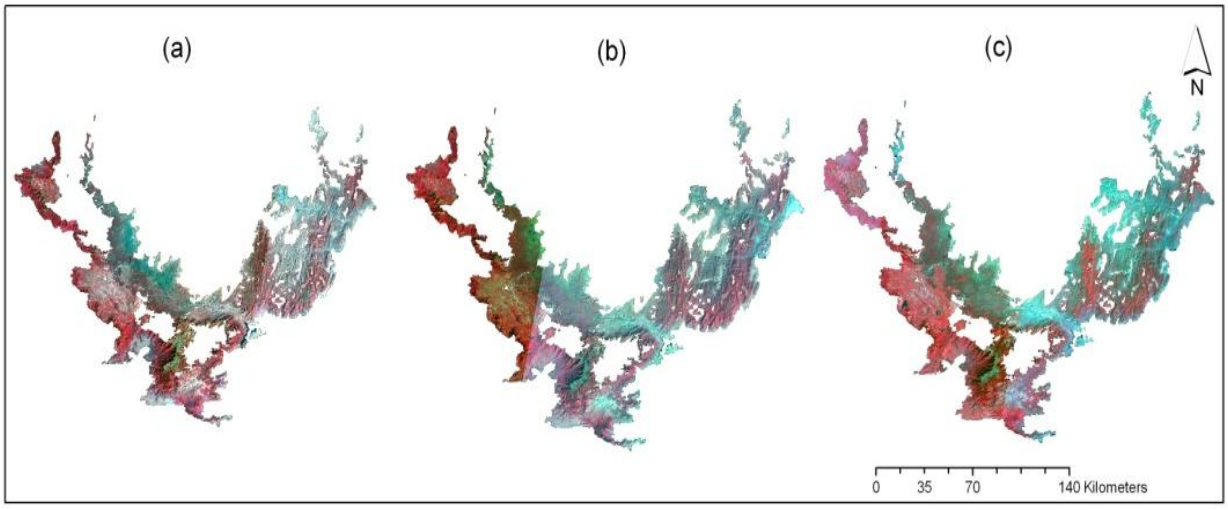

Figure 2.3: Map showing False Colour Composite (FCC) of the study area for a) 1973 b) 1992 and C) 2011.

2.3. Results and Discussion

2.3.1. Land use and Land cover classification

The confusion matrixes and accuracy measures of supervised classification can be found in Tables 3, 4 and 5. The overall classification accuracy for 1973 is 42.7% with overall Kappa Statistics = 0.354, 43.5% for 1992 with overall Kappa Statistics = 0.359 and 55.6% for 2011 with Overall Kappa Statistics = 0.502.

The uncertainty of the classified thematic maps with high degree of error can be the outcome of differences in dates of data acquisition within a landscape, different preprocessing techniques and reliability of expert knowledge. Figure 2.3 shows the FCC composite of the study area. In the year 1973, large areas devoid of vegetation can be seen, which seem to be due to clearing of vegetation for planting coffee, tea, teak, rubber and food crops. These newer vegetation elements can be seen in the classified imagery of later years. The landscape also seems to have experienced regular fires in the earlier years but in 2011 the extent of fire was lower because of active fire control measures in the area. Table 2.3 shows the different codes generated during the classification for the different years.

Table 2.3: Codes for land use and land cover classes for different years

SL.No.	1973	Code	1992	Code	2011	code
1	Settlement	1	Plantation	5	Coconut/banana	2
2	Shadow	2	Water Bodies	7	Tea	3
3	Barren Land	3	Wet Evergreen	9	Moist Deciduous	4
4	Cloud	4	Settlement	11	Dry Evergreen	5
5	Dry Thorn	5	Tea	14	Settlement	6
6	Dry Deciduous	6	Coconut/banana	15	Cloud	8
7	Water Bodies	7	Barren land	17	Coffee	9
8	Grassland	8	Dry Deciduous	26	Shadow	13
9	Burned Area	9	Cloud	27	Dry Thorn	14
10	Plantation	11	Shadow	28	Barren land	17
11	Dry Evergreen	12	Dry Evergreen	37	Agriculture	31
12	Agriculture	22	Moist Deciduous	40	Dry Deciduous	42
13	Coffee	31	Grassland	41	Plantation	48
14	Tea	34	Agriculture	44	Wet Evergreen	79
15	Wet evergreen	53	Burned	48	Grassland	84
16	Moist Deciduous	77	Coffee	49	Water bodies	189
17	Settlement	0	Dry Thorn	63	Burned area	0

Table 2.4: Confusion matrix for supervised classification of 1973

Classes	Coconut	1	2	3	4	5	6	7	8	9	11	12	22	31	34	53	77	Row Total
Coconut	0	0	0	0	0	0	0	0	0	0	0	0	0	0	0	0	0	**0**
1	0	0	0	0	0	0	0	0	0	0	0	0	0	0	0	0	0	**0**
2	0	0	0	0	0	1	5	0	2	0	0	0	0	0	0	2	0	**10**
3	0	0	0	3	0	7	5	1	1	0	0	0	3	0	0	0	3	**23**
4	0	1	0	0	0	0	1	0	1	0	0	0	1	0	0	0	0	**4**
5	18	3	0	11	0	53	15	3	1	0	6	1	9	0	0	2	5	**127**
6	0	2	0	4	0	51	154	6	8	0	11	14	4	0	0	4	68	**326**
7	0	0	0	4	0	2	1	26	0	0	0	0	3	0	0	0	1	**37**
8	0	0	0	2	0	5	6	5	20	0	3	1	0	0	1	13	3	**59**
9	0	0	0	0	0	3	43	1	0	0	1	0	1	0	0	1	4	**54**
11	5	1	0	2	0	1	1	0	3	0	18	0	2	4	7	7	9	**60**
12	0	0	0	0	0	1	1	0	0	0	0	2	0	0	0	0	4	**8**
22	19	12	0	8	0	14	8	5	3	0	11	0	85	3	0	3	4	**175**
31	1	7	0	5	0	0	1	5	0	0	4	0	37	53	7	5	4	**129**
34	1	0	0	0	0	0	0	0	1	0	0	0	1	3	17	2	3	**28**
53	1	2	6	3	0	1	3	6	12	0	5	0	16	8	8	92	17	**180**
77	1	1	1	0	0	9	34	5	1	0	15	1	2	3	1	4	56	**134**
Column Total	**46**	**29**	**7**	**42**	**0**	**148**	**278**	**63**	**53**	**0**	**74**	**19**	**164**	**74**	**41**	**135**	**181**	**1354**

The total sample points used for the accuracy assessment in the confusion matrix for the different years are different due to mismatches with ground locations, or not used for assessment accuracy (Tables 2.4, 2.5 and 2.6). The accuracy is measured by how many points in an area are correctly classified with the ground sample points.

Table 2.5: Confusion matrix for supervised classification of 1992

Classes	5	7	9	11	14	15	17	26	27	28	37	40	41	44	48	49	63	Row Total
5	16	0	7	2	3	1	1	5	0	0	0	12	0	2	0	3	0	**52**
7	0	35	0	0	0	0	2	1	0	0	0	0	0	0	0	0	2	**40**
9	6	3	78	2	7	1	0	8	0	5	7	20	9	4	0	13	1	**164**
11	0	1	2	1	0	1	0	1	0	0	0	1	0	4	0	0	2	**13**
14	2	0	2	1	21	1	0	0	0	0	0	2	2	1	0	3	0	**35**
15	1	1	4	0	0	2	0	0	0	0	0	0	0	2	0	0	0	**10**
17	0	1	0	0	0	2	6	4	0	0	0	0	0	9	0	0	3	**25**
26	9	3	3	2	0	5	2	178	0	1	7	70	8	10	0	0	50	**348**
27	1	0	1	1	0	4	1	0	0	0	0	0	0	1	0	0	0	**9**
28	0	0	1	0	0	0	1	10	0	1	0	6	5	0	0	0	4	**28**
37	3	0	3	0	1	0	0	1	0	0	2	1	2	0	0	0	0	**13**
40	15	3	12	1	0	16	2	29	0	0	2	51	7	2	0	2	12	**154**
41	8	1	6	1	0	0	1	0	0	0	0	0	11	4	0	0	1	**33**
44	7	4	7	12	5	13	10	7	0	0	0	11	3	91	0	12	13	**195**
48	0	2	0	0	0	0	0	4	0	0	0	0	2	0	0	0	3	**11**
49	6	5	8	4	4	1	3	0	0	0	0	3	0	23	0	41	0	**98**
63	1	5	1	2	0	0	13	31	0	0	1	5	4	9	0	0	56	**128**
Column Total	**75**	**64**	**135**	**29**	**41**	**47**	**42**	**279**	**0**	**7**	**19**	**182**	**53**	**162**	**0**	**74**	**147**	**1356**

Table 2.6: Confusion matrix for supervised classification of 2011

Classes	2	3	4	5	6	8	9	13	14	17	31	42	48	79	84	189	Row Total
2	17	0	8	0	1	0	0	0	0	0	3	0	5	2	1	0	**37**
3	1	22	3	0	0	0	3	0	0	0	1	0	3	3	1	0	**37**
4	11	1	78	5	0	0	5	0	15	2	2	40	8	11	5	1	**184**
5	0	0	12	10	0	0	0	0	3	0	1	7	0	0	2	0	**35**
6	0	0	0	0	3	0	0	0	0	1	4	0	0	0	0	0	**8**
8	0	0	0	0	0	0	0	0	0	0	1	0	0	1	0	0	**2**
9	0	6	0	0	4	0	56	0	0	0	17	0	4	4	2	1	**94**
13	0	0	2	0	0	0	0	2	3	1	0	8	0	1	2	1	**20**
14	1	0	8	0	3	0	0	0	85	9	4	42	1	0	2	0	**155**
17	1	0	0	0	1	0	0	0	1	15	11	2	1	1	2	0	**35**
31	5	1	2	0	11	0	7	0	8	8	101	9	2	4	4	3	**165**
42	2	0	43	0	0	0	0	1	27	0	3	160	4	2	0	4	**246**
48	3	2	11	0	2	0	1	0	1	2	2	6	44	9	2	1	**86**
79	6	9	14	3	2	0	2	4	1	0	10	1	2	91	10	2	**157**
84	1	0	0	1	2	0	0	0	1	1	3	4	0	6	19	0	**38**
189	0	0	1	0	0	0	0	0	3	2	0	0	0	0	1	52	**59**
Column Total	**48**	**41**	**182**	**19**	**29**	**0**	**74**	**7**	**148**	**41**	**163**	**279**	**74**	**135**	**53**	**65**	**1358**

However, the lower accuracy in classification for 1973 and 1992 as compared to 2011 may also reflect more changes in the landscape during the earlier periods. Spatial and spectral resolution of the satellite sensor influences the quality of classification; higher resolution of images for 2011 may also have resulted in higher accuracy. The Kappa Statistics was also different for the classification accuracies of the different years.

2.3.2. Spatial distribution of land use and land cover

The study area supports all the major vegetation types of peninsular India (Champion and Seth 1968).These includes tropical evergreen and semi-evergreen forest, tropical moist deciduous forest, tropical dry deciduous forest and tropical dry thorn forest.

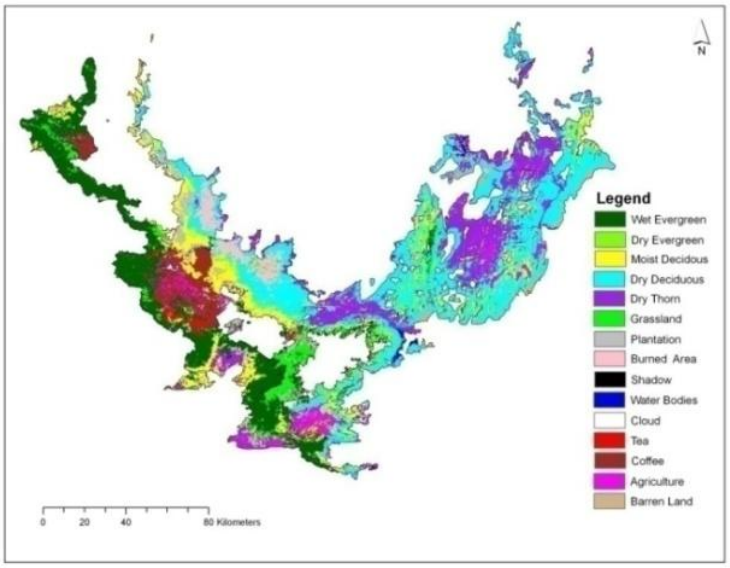

Figure 2.4: Land use /land cover map of 1973

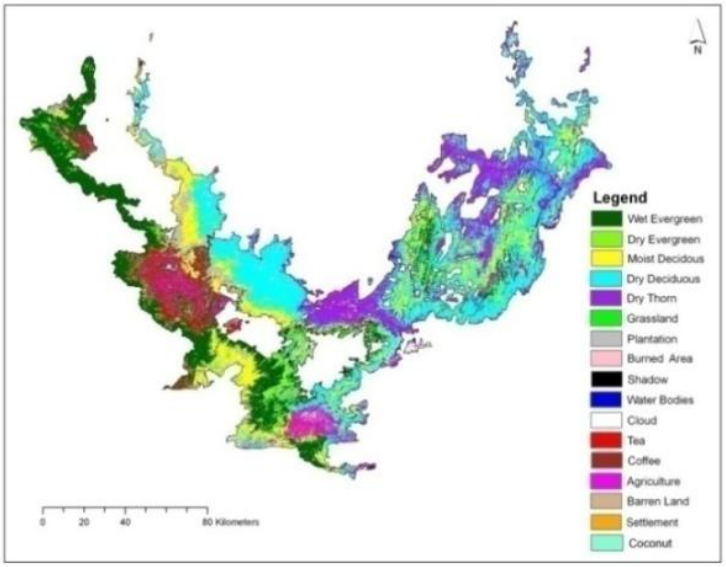

Figure 2.5: Land use/land cover map of 1992

At higher altitudes (>1800 m) there is also a characteristic association of two vegetation types, namely, patches of tropical montane stunted evergreen forest (locally called *shola*) in the valleys and folds of the hills, and extensive grassland on the hill slopes. Apart from natural vegetation types, the human-dominated mosaic includes agriculture, plantations of coffee/tea, coconut/banana, and settlements. Figure 2.6 provides the current spatial pattern of the LULC in the study area. We have included forest areas contiguous to Elephant Reserves 7 and 8 to facilitate an understanding of not only forest types but also movement of animals across the entire landscape.

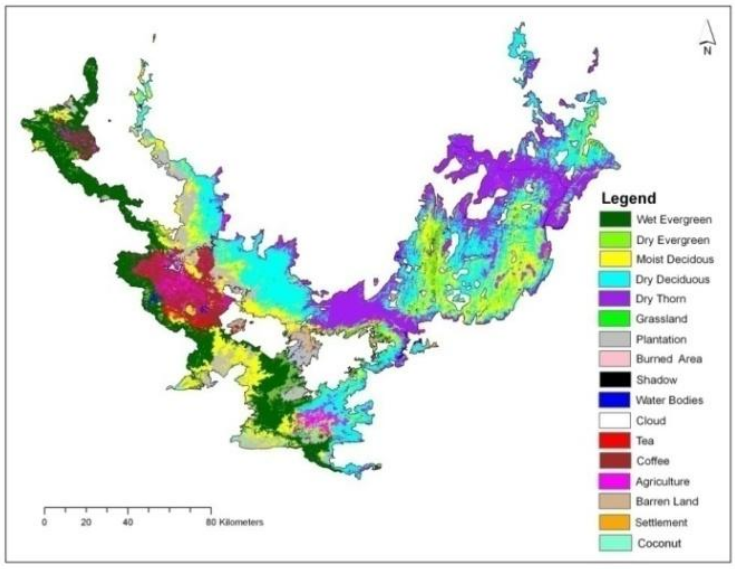

Figure 2.6: Land use and land cover of 2011

Table 2.7: Land use/Land cover area statistics (square kilometer and percentage of total)

	Year	1973		1992		2011	
Land use/Cover categories	**ID**	**Area in km^2**	**Area in %**	**Area in km^2**	**Area in %**	**Area in km^2**	**Area in %**
Agriculture	1	845.57	5.58	891.55	5.89	613.37	4.04
Barren Land	2	329.52	2.17	156.02	1.03	119.59	0.79
Burned Area	3	550.84	3.63	126.51	0.84	0.00	0.00
Cloud	4	29.47	0.19	86.23	0.57	0.38	0.00
Coconut	5	0.00	0.00	30.13	0.20	83.36	0.55
Coffee	6	760.76	5.02	698.08	4.61	746.08	4.92
Dry Evergreen	7	133.67	0.88	147.75	0.98	221.29	1.46
Dry Deciduous	8	4534.22	29.91	4437.26	29.30	3907.21	25.75
Dry Thorn	9	1965.39	12.96	2232.05	14.74	2892.25	19.06
Grasslands/Sholas	10	581.0 9	3.83	382.83	2.53	461.62	3.04
Moist Deciduous	11	1866.51	12.31	2300.33	15.19	2367.52	15.60
Plantation	12	574.06	3.79	619.67	4.09	1184.23	7.81
Settlement	13	0.00	0.00	61.14	0.40	21.62	0.14
Shadow	14	97.54	0.64	189.09	1.25	26.62	0.18
Tea	15	78.30	0.52	96.12	0.63	86.90	0.57
Water Bodies	16	138.90	0.92	96.07	0.63	109.27	0.72
Wet evergreen	17	2673.98	17.64	2592.70	17.12	2330.29	15.36
Total Area		**15143.52**	**100.00**	**15143.52**	**100.00**	**15171.61**	**100.00**

Table **2.7** shows the statistics of different land use and land cover type derived for the three time periods. The percentage of agriculture and barren land decreased over time but this might be due to the expansion of commercial plantations and possibly coconut groves (though this may be an erroneous result as we failed to distinguish any land use under coconut in the low resolution 1973 image). Dry thorn forest as well as moist deciduous forest seems to have increased over time.

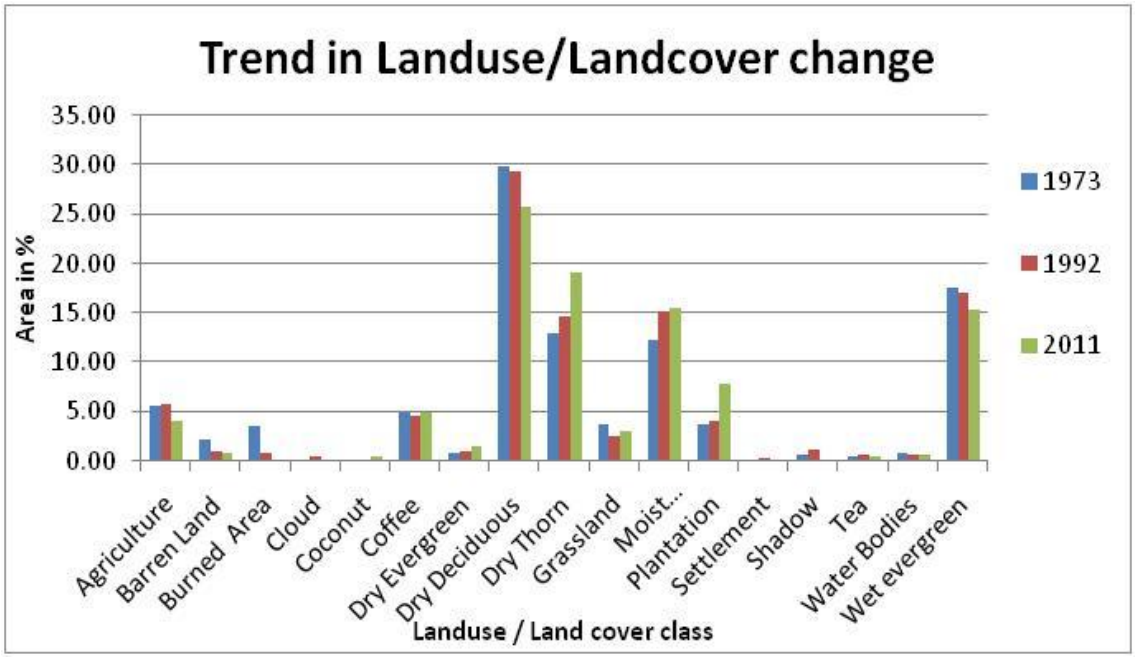

Figure 2.7: Land use and land cover change in percentage

No conclusions can be drawn from this analysis about trends in burned area because fires are not only highly seasonal but also show much inter-annual variation; snapshots of three years are insufficient to infer trends. Area under coffee remained almost the same through the analysis but area under tea increased substantially. Moist deciduous forest increased from 12% to 15%; this might be due to misclassification of wet evergreen forest as well as the difficulty in distinguishing spectral signatures of dry deciduous and moist deciduous forest. Major changes have taken place outside the natural forested regions. The large increase in area under dry thorn forest may partly be due to misclassification of dry deciduous forest that has further dried. Large areas were planted with rubber, eucalypts, wattle and teak after the 1970s, whereas wet evergreen forest experienced decreased in area.

2.4. Conclusions

The study reveals temporal changes in land use and land cover over a period of 38 years captured during 1973, 1992 and 2011. Comparisons of thematic maps produced from remote sensing data show that the area under dry thorn forest, moist deciduous forest, coffee, tea and coconut had increased. On the other hand, there is reduction in area under agriculture barren land, wet evergreen forest, burned area and grasslands/sholas. The comparative analysis of land use and land cover suggests that there is no visible improvement in forest status. The spatial extent and distribution of vegetation types can be linked to human-induced changes. High resolution, multi-temporal, satellite data on LULC can be used for evaluating the current status of forests and extent of change for future planning, policy and forest management.

Chapter 3

Developing maps of forest degradation in the Nilgiri Biosphere Reserve

3.1 Introduction

Mapping, quantifying, and monitoring changes in the physical characteristics of forest cover is one of the most important elements in the study of global change (Nemani and Running, 1996). Forested ecosystems actively regulate biosphere dynamics through contributions to the carbon and nitrogen cycles, the hydrological cycle and the surface energy balance (Choudhury, 1987). However, disturbances in a forested region require extensive investigation of rate of change in vegetation structural characteristics (Halim et al., 2008). Researchers are developing new methods and technologies to monitor forest cover change and to estimate changes in carbon stocks over time in various parts of the world (Asner et al., 2009).

Much of the research in the tropics has focused on deforestation or static evaluations of forested areas, but seldom have they considered the contributing effects of landscape ecological processes and biotic pressures in the loss of biodiversity (Das et al., 2006). Although they have been studied separately to varying degrees, the combined ecological impacts of forest fragmentation, in unison with biotic pressures such as grazing, logging, and forest fires, are poorly understood. Studies in the Western Ghats have indicated a three-fold increase in fire frequencies over the past century (Kodandapani et al., 2004). Similarly, studies have recorded a proliferation of invasive plant species such as *Lantana camara* in southern India (Hiremath and Sundaram, 2005; Ramaswami and Sukumar, 2013). The Nilgiri landscape has also shown increased pressures on forests from adjoining human habitations (Lo Seen et al., 2010).

The Normalized Difference Vegetation Index (NDVI) has been used extensively for studying the variation in spatial and temporal changes of vegetation across different scales (Tucker, 1979). NDVI also has the problem of background spectral variability of soil albedo which affects the relationship between NDVI and vegetation (Huete, 2002). Spectral Mixture Analysis (SMA) helps to detect the percentage of land use/land cover in each pixel by unmixing technique (Rashed et al., 2001; Dawelbait and Morari, 2011). Change vector analysis (CVA) is used to detect the change in magnitude and direction between the two (spectral) input images for each date (Malila, 1980; Lambin and Strahler, 1994). The Nilgiri Biosphere Reserve (NBR) is spread over the states of Karnataka, Kerala and Tamil Nadu. The region supports all types of vegetation types and is under human pressure due to developmental activities over the years both within and outside the reserve. Here we evaluate methods to map the degree of forest degradation in the Nilgiri Biosphere Reserve (NBR) and adjoining areas constituting Elephant Reserves 7 and 8.
The main aim of the study is assess the disturbances of the landscape using multi-temporal remote sensing data with SMA and CVA techniques.

3.2. Materials and Methods

3.2.1. Dataset and preprocessing

Landsat MSS Dataset of 1973 and Landsat TM of 1992 were downloaded from NASA https://earthexplorer.usgs.gov/ while IRS LISS III P6 satellite data for 2011 was procured from National Remote Sensing Centre, Hyderabad, in digital format. Details about the datasets used in study are mention earlier in chapter 2. All the images from Landsat MSS, TM and IRS were subjected to preliminary processing such as atmospheric and geometric corrections. The 2011 image was georectified using 1:250000 Survey of India (SOI) topographic maps. The root mean square (rms) error was <0.50 pixel. The other images were geo-registered using 2011 image with image to image georegistration technique. Spatio-temporal change detection process involves determining the changes in land use and land cover with multi-temporal remote sensing data. The capability of capturing changes and extracting information about changes from satellite data requires effective change detection techniques. All data sets have to be brought on to a common platform before further analysis by doing resampling at 24 m spatial resolution.

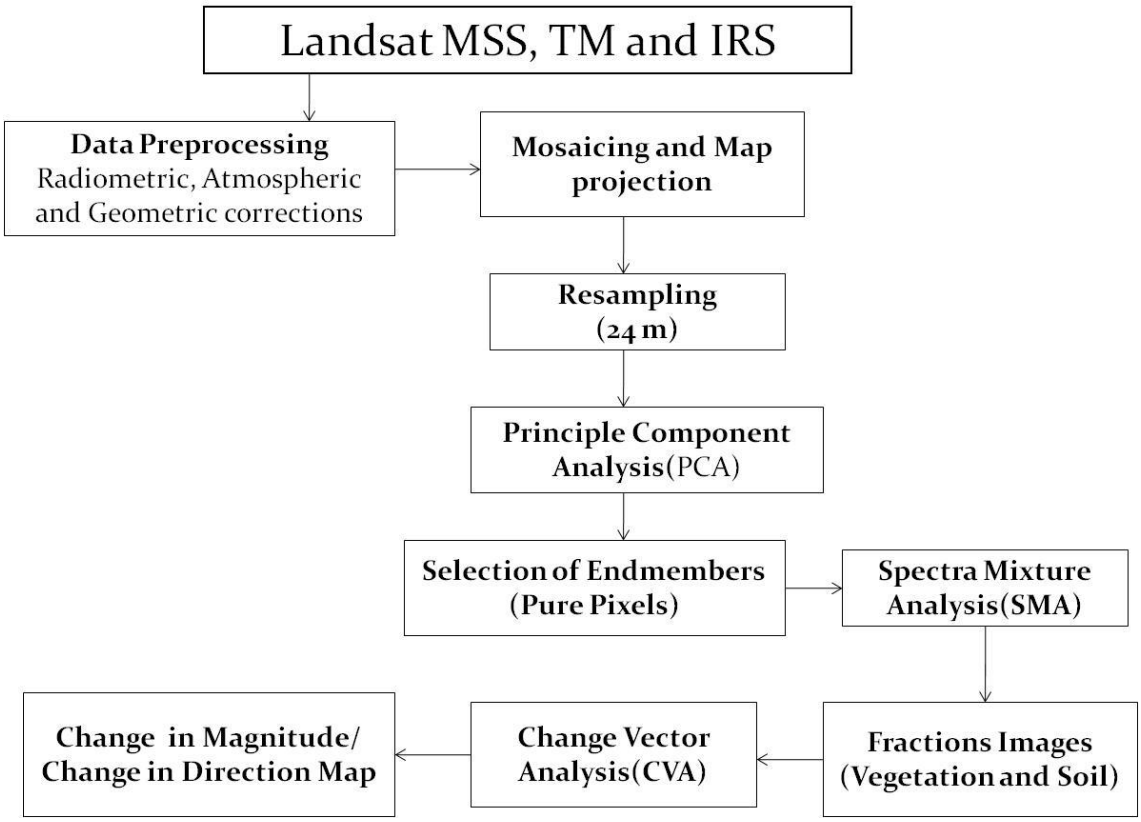

Figure 3.1: A flow chart showing the methodology followed.

3.2.2. Spectral Mixture Analysis and Endmembers

Before applying SMA to remote sensing images, Principal Components Analysis PCA was used to select the pure pixels with 100% cover as endmember. Each endmember can be plotted to identify the pixels with pure endmember located at the corners on a scatter plot. The fraction images with associated RMSE images were produced using different endmembers (Elmore et al., 2000). Fraction images generally represent the mixing proportions of different endmember spectra (Adams et al., 1986). SMA technique involves three steps (Huete et al., 2004): a) assess the dimensionality or number of endmembers with unique reflecting materials in a landscape; b) to identify within a pixel the physical nature of each endmember; c) to determine the amounts of each endmember within each pixel. In order to understand the spatial and ecological processes of landscape change in the study area, the baseline data were created using spectral mixture analysis with satellite imagery. For performing the spectral mixture analysis, three end members were chosen, namely, photosynthetic vegetation, soil, and shade.

3.2.3. Change Vector Analysis

The output results from the Spectral Mixture Analysis were used to perform Change Vector Analysis for detecting change in magnitude and direction of forest degradation. SMA (Lu et al., 2005; and Moran, 2004) and CVA (Dawelbait and Morari, 2011) is used to evaluate the variation in land use and land cover (LULC). Three endmembers i.e. vegetation, soil and shade were applied to SMA in order to produce the fractions with associated RMSE images. CVA allows measuring the magnitude and direction of change between two dates. Vegetation and soil fraction images were used for CVA. Thus, coincident pixels were analyzed in pairs of two time periods using the fractions images and the angles were computed using the following formula (Kuzera et al., 2005).

$$R= \sqrt{(x1 - x2)2 + (y1 - y2)2} \quad \text{----------equation 1}$$

Where, R is the Euclidean Distance
x1 is soil fraction in time 1;
x2 is soil fraction in time 2;
y1 is vegetation fraction in time 1;
y2 is vegetation fraction in time 2

3.2.4. Change Detection

To evaluate the variation in land use and land cover (LULC) two methods were used. The first method was visual interpretation of the different land cover elements in the satellite images. Visual interpretation for each endmember was performed by displaying fractions images of the

three years 1973, 1992 and 2011, and rescaling from 0 to 255 into percentage scale. The other method used for the change detection was Change Vector Analysis (CVA) (Malila, 1980; Chen et al. 2003). The changes between the two periods can be evaluated by CVA which allows the direction and magnitude of change to be detected. Fraction images of vegetation and soil were used to monitor the regeneration and degradation of vegetation for the three time periods (1973-1999, 1992-2011 and 1973-2011). Change direction was measured by the angle of the change vector between the difference of the position of the same pixel in two different years. Angles which measured between 90° and 180° indicated an increase in bare soil and decrease in vegetation, and therefore an increase in degraded area. On the other hand, angles measured between 270° and 360° indicate a decrease in bare soil and an increase in vegetation. The angles measuring between 0°-90° and 180°-270° indicate either increase or decrease in both vegetation and soil which can be considered as persistence (Khiry, 2007). Change of magnitude is measured as the Euclidean distance or length of the change vector between two coincident pixels measured in the two different years (see equation 1 above). The four classified classes of magnitude represent the level of degradation or re-growing with persistence (Kuzera et al., 2005).

3.2.5. Ground truth data:

Twenty-two 30m x 30m plots were sampled in different forest types in the Nilgiri Biosphere Reserve. Data on percentage vegetation cover such as the grasses, invasive species, and tree species (≥ 10 cm dbh) density were collected in nine subplots of 10m x 10m within each of the larger plots. GPS locations of the four corners of the plots were collected. In addition, anecdotal information such as the occurrence of fire was also gathered.

3.3. Results and Discussion

In this study SMA and CVA techniques were applied to different datasets of Landsat MSS, TM and IRS images. Three derived endmembers of vegetation, soil and shade were produced. The SMA model was used to characterize the landcover types into fraction images. The CVA was used to map the change vector magnitude intensity of changes betweens pixel's vegetation (greenness) and soil (openness). CVA was also used to produce the change in vector direction in vegetation and soil. The study period was determined by computing the differences in fraction images. Field data were collected to validate the fractions images with vegetation and soil from the actual ground.

3.3.1. Spectral Mixture Analysis

In Figure 3.2, fraction images of vegetation are shown for the years a) 1973 b) 1992 and c) 2011 where the colour ranges from red to green as a percentage of vegetation cover in each pixel. In the bottom, the fraction images of soil are shown for the year d) 1973 e) 1992 and e) 2011 where

the colour ranges from red to blue as a percentage of soil cover in each pixel which is showing 1-100% which is rescaled to 1-10 at each pixel.

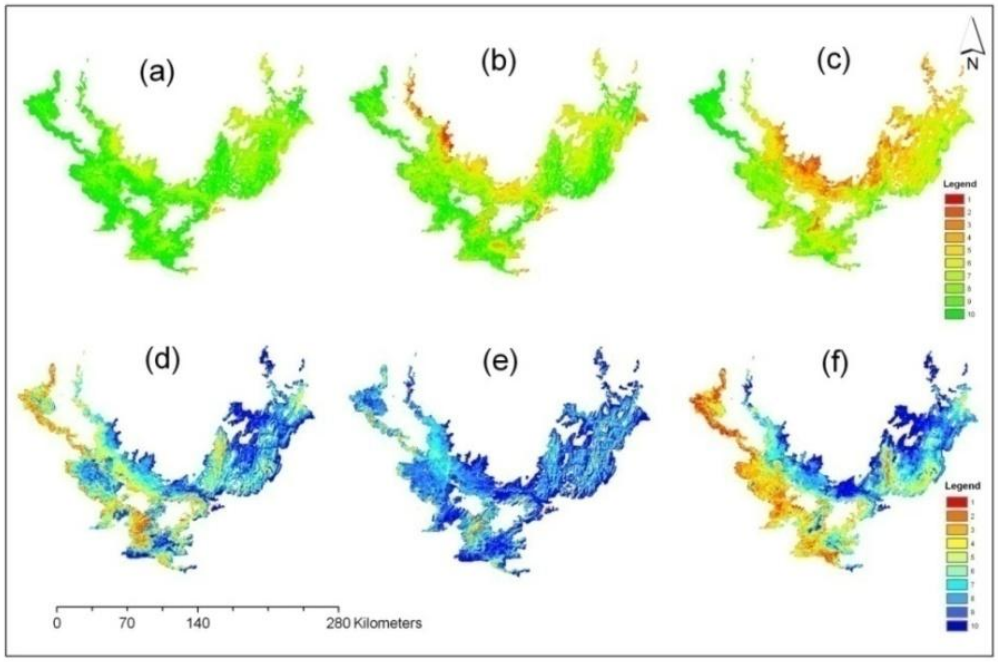

Figure 3.2: Fraction images of vegetation (top) and soil (bottom)

Table 3.1: Fraction cover values extracted from ground data with vegetation type.

Plot Id.	veg_73	veg_92	veg_11	soil_73	soil_92	soil_11	Green Cover	Vegetation Type
1	8	6	4	10	10	6	10	Dry Deciduous
2	7	6	3	10	10	9	10	Dry Thorn
3	9	9	8	6	9	6	10	Dry Deciduous
4	6	5	1	7	9	10	10	Dry Thorn
5	6	5	2	6	9	8	8	Dry Thorn
6	8	2	1	7	6	10	8	Dry Thorn
7	8	6	1	7	9	8	10	Dry Deciduous
8	10	8	4	6	10	7	10	Moist Deciduous
9	5	2	2	10	10	10	10	Grassland
10	10	9	2	5	10	8	10	Dry Deciduous
11	8	6	5	7	8	7	10	Dry Deciduous
12	10	7	4	5	7	6	5	Dry Deciduous
13	9	7	4	6	10	7	10	Moist Deciduous
14	10	8	3	5	8	8	9	Moist Deciduous
15	7	6	3	4	6	6	10	Moist Deciduous
16	8	6	2	7	8	9	9	Moist Deciduous
17	5	6	3	7	8	8	10	Dry Deciduous
18	6	2	1	6	10	10	10	Dry Decidious
19	6	5	3	7	8	9	10	Dry Deciduous
20	10	6	3	6	9	8	10	Dry Deciduous
21	9	7	4	8	9	7	10	Dry Deciduous
22	8	7	3	5	8	9	10	Dry Deciduous

The percentage of vegetation was determined for different years and fraction value (of vegetation) extracted at each pixel for the plots (**Table 3.1**). In general, we tried to establish the relationship between SMA fraction and ground percentage of green cover in the plot but were unable to do so as the survey was done in the month of October which is an overestimation of the percentage of green cover from the ground data. The soil estimated was done for the January to March dry season. This overestimate may due to the mis-registration of multi-date scenes used and sites located in the field. It is believed to be the largest source of errors in the SMA fraction for making comparison for different years (Brandt et al. 2006).

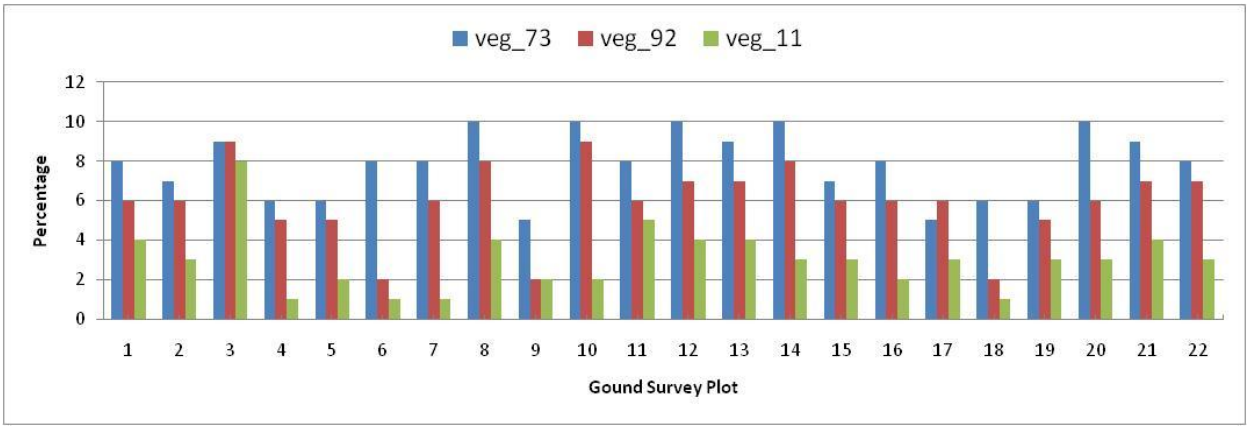

Figure 3.3: Vegetation fraction cover of each pixel located in the ground survey plots

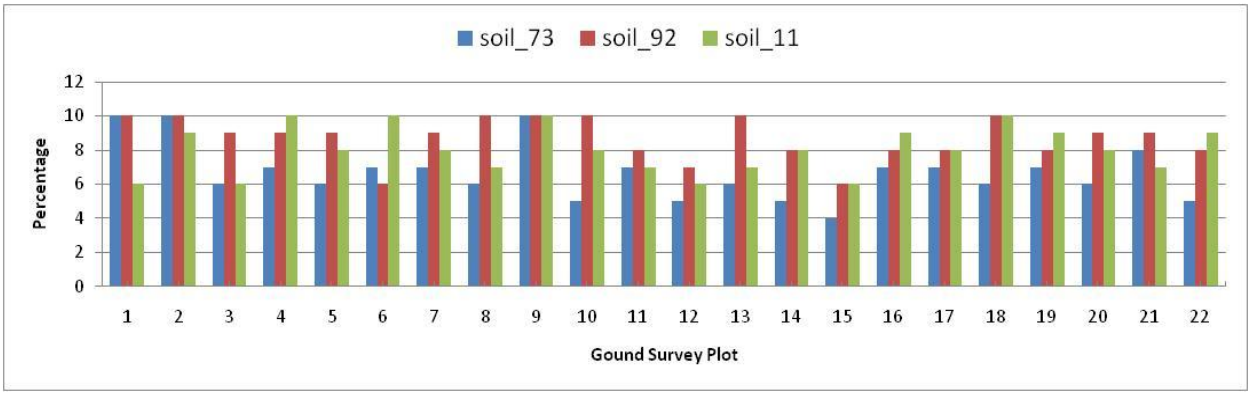

Figure 3.4: Soil fraction cover of each pixel located in the ground survey plots

The vegetation cover for the year 1973 was high as compared to 2011 (Figure 3.3), but vegetation phenological differences during the dates of satellite data acquisition between the two years could have partly contributed to the difference in classified forest cover. The deciduous forest area seems to have expanded between 1973 and 2011. Out of our 22 experimental plots, 11 plots have shown extended bareness (openness) of canopy from year 1972 to 2011. Both the observations from satellite data and ground truth revealed that the forest canopy is opening (Figure 3.4).

3.3.2. Change Vector Analysis

3.3.2.1. Analysis of the changes in fraction images 1973-1992

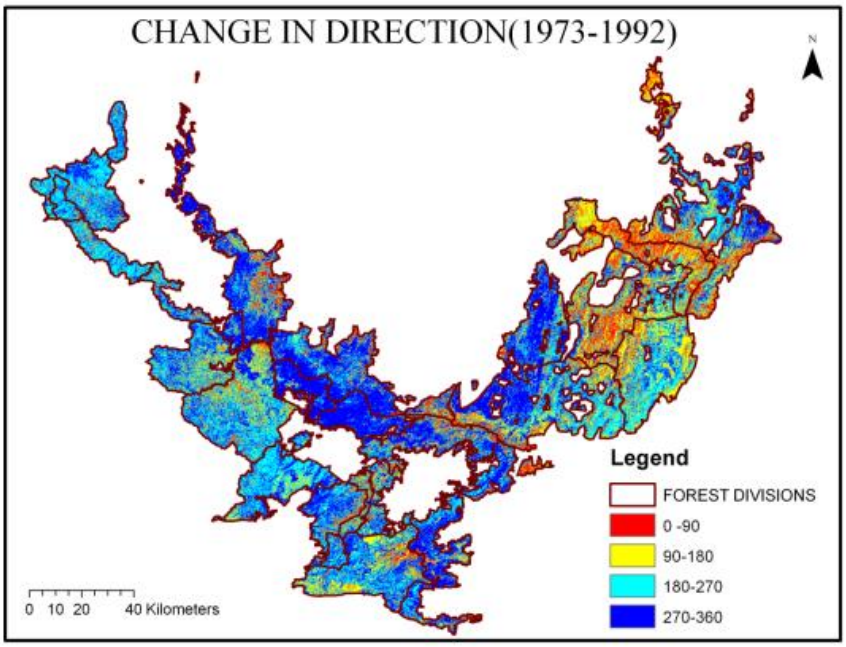

Figure 3.5: Forest degradation and forest regeneration areas calculated by applying CVA from 1973 to 1992

CVA quantified the changes in fraction of vegetation and soil between the years 1973 and 1992 (Fig. 3.5). There seems to be an increase in vegetation in areas where denser forest is found which is shown in yellow colour but, in areas with agriculture, plantation, low lying areas along the hill slopes and in eastern part of the landscape, there seems to be degradation which is shown in yellow colour. During 1973-1992 expansion of plantations was carried in areas in areas like Wyanad, Nilambur, and Nilgiris. During the same period, protected areas such as Mudumalai carried out selective felling of timber while Nagarahole and Nilambur converted natural forest to teak plantation. Revenue lands under forest in Mannarghat were brought under intensive agriculture and horticulture (Prabhakar, 1994) (see also Appendix 6). However, the greatest negative changes seem to have taken place in the Eastern Ghats, in areas such as the (later designated) Cauvery Wildlife Sanctuary, Bannerghatta, Kollegal and Erode Forest Division.

3.3.2.2. Analysis of the changes in fraction images 1992-2011

During the period 1992-2011 there seems to be a decrease in vegetation in most of the areas where dense forest was found in 1992 and an increase in biomass in many areas where degradation was seen during 1973-92 (Fig. 3.6), thus following an opposite trend to what was

experienced earlier. During this period, more than 60% of the area remained unchanged, while major negative changes seem to have taken place in Madikeri Territorial, Hunsur Wildlife, Wyanad North, Wyanad South, Mannnarghat, Coimbatore, Nilgiri North, and Dharmapuri Forest Divisions (Appendix: 6). Major expansion of tea, coffee, settled agriculture and horticulture took place during this period in Wyanad, Mannarghat and the Nilgiris (Prabhakar 1994). The hill slopes and eastern part of the landscape, basically the drier areas, generally experienced increase in biomass and areas under moist deciduous and evergreen forest remain relatively unchanged. This period (1992-2011) marks a phase of consolidation of existing forests after enactment of the Forest Conservation Act (1980).

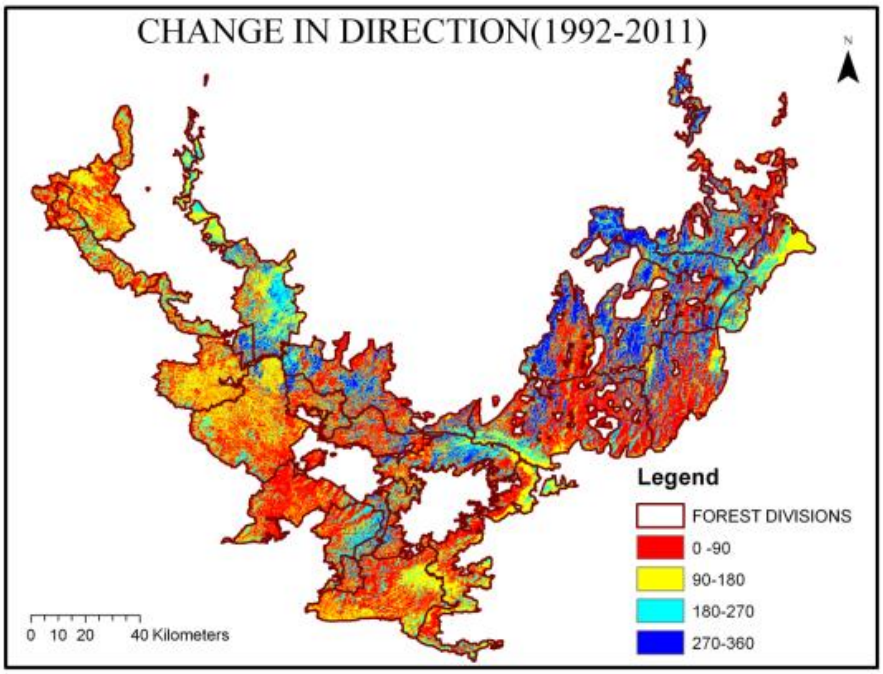

Figure 3.6: Forest degradation and regeneration areas calculated by applying CVA from 1992 to 2011

3.3.2.3. Analysis of the changes in fraction images 1973-2011

The long term directional change was quantified for the 38-year time period (**Fig 3.7.)**. There seem to be increase in vegetation in forested areas of the regions which are declared protected reserve forest across a wide area from Nagarahole, through Bandipur, Mudumalai and BRT Sanctuary (Appendix **6 :**). But this positive trend might be also due in part to the increase of the invasive species *Lantana camara* over years across the deciduous forests of these protected areas (Ramaswami and Sukumar, 2013). The most visible negative changes in biomass are seen in Wyanad North and Wyanad South Forest Divisions possibly due to conversion agriculture, tea, coffee, other plantations and horticulture during this period (1973-2011).

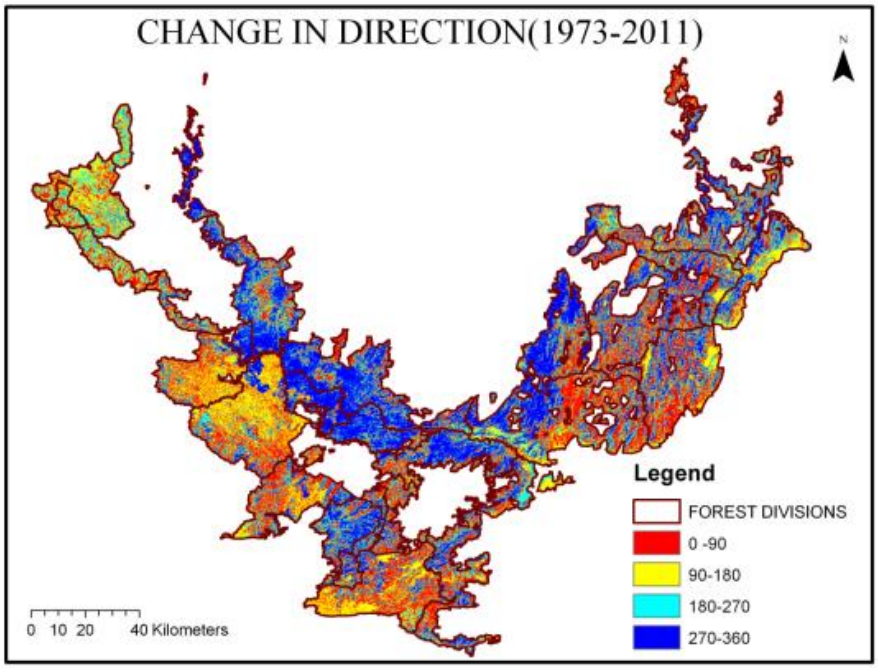

Figure 3.7: Forest degradation and forest regeneration areas calculated by applying CVA between 1973 and 2011

Table 3.2: Degradation and regeneration of forest status from 1973 to 2011

Year	1973-1992		1922-2011		1973-2011	
Status of Forest	Area in sq km	Area in %	Area in sq km	Area in %	Area in sq km	Area in %
Persistence(0-90)	3716	25	7598	50	6509	43
Degradation(91-80	1068	7	3269	22	2159	14
Persistence(181-270)	2757	18	1690	11	687	5
Regeneration(271-360)	7589	50	2573	17	5775	38
Total	15130	100	15130	100	15130	100

Table 3.2 shows the different extent of directional changes in the landscape. During 1973-1992, 7% of the area falls into the category of degradation, a figure which increased to 22% during 1992-2011. In case of the regeneration category it decreased from 50% of 1973-1992 to 17%. For the net effect during the time period 1973-2011, about 48% of the area persisted in the same state, while 38% of the area regenerated (improved in status) and 14% of the land degraded (declined in status).

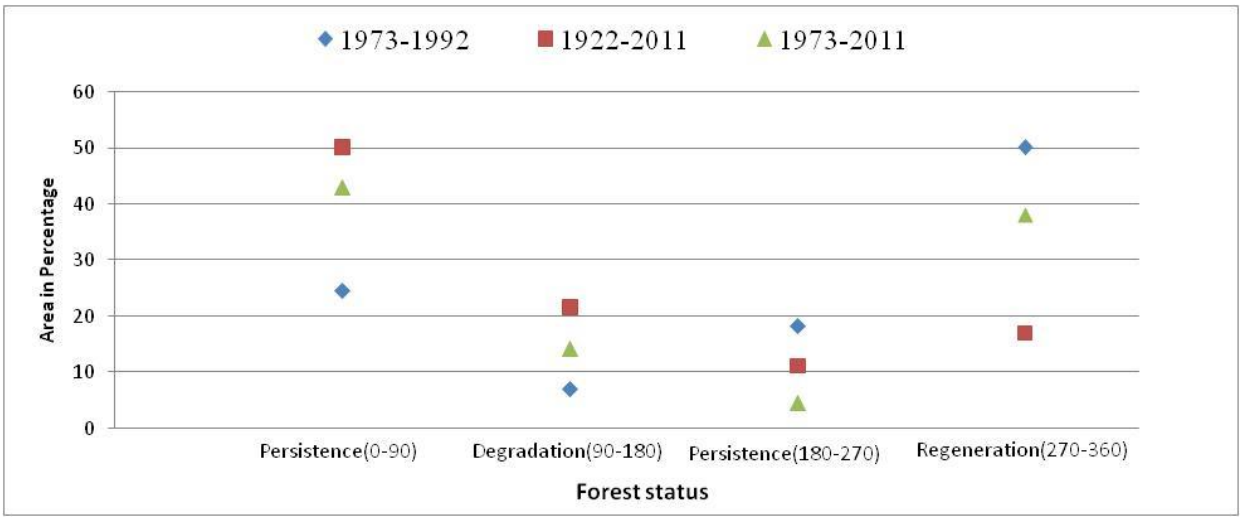

Figure 3.8: Forest degradation and forest regeneration area in percentage 1973 to 2011

The above figure shows different levels of forest status where the lowest level of degradation was found in 1973-1992 and highest level in 1992-2011. The highest level of regeneration was also found for 1973-1992 and lowest in 1992-2011.

3.4. Conclusions

These results showed the capability of CVA to detect historical changes in vegetation gain and loss across a landscape. The dynamical nature of a landscape is measurable through the direction and magnitude of change. During the decade of the 1970s, the landscape continued to be exploited for natural resources and land use conversion was common. Since 1980 an effort was made to conserve forests through legal means. This is reflected in an overall increase in biomass in the drier areas of the landscape under deciduous forest cover and given protected area status; however there are good reasons to believe that this increase in biomass was partly due to the expansion of an invasive woody plant *Lantana camara*. The other interesting observation, which also has management implications, is that the wetter western parts of the landscape have overall degraded with loss of biomass. While some of this could be due to land-use change, the possibility of factors relating to climate change in this transformation cannot be ruled out.

Chapter 4

Ecological Responses of Environmental Changes

4.1. Introduction

Forests play an important in maintaining the biodiversity of a region (McDermid et al., 2005; Yadav et al., 2012). Forests also regulate climate, carbon and nitrogen cycles (Nemani and Running, 1996), and hydrologic functions. Evapotranspiration rates and surface runoff volumes can also be altered in a forested landscape (Schmugge et al., 2002). With the increase in human population the pressure on different lands for natural resources has increased over time. Resource extraction has often resulted in the loss of forested land cover, leading to impacts on biodiversity from habitat conversion (Cuba et al., 2013).

Vegetation indices have a long historical application in evaluating forest cover using spectral measurements (Bannari et al., 1995) which are used for quantitatively and qualitatively understanding vegetation properties such as greenness, biomass, stress, and density (Mašková et al., 2008). Normalized Difference Vegetation Index (NDVI) is the most commonly used index for comparing and analyzing quantitative changes in vegetation over time (Herrmann et al., 2005; Pettorelli et al., 2005).

Despite the influence of vegetation phenology (Jeganathan et al., 2010), moisture content, differences in the wavelength of sensors, view angle of sensor, and the sun's zenith angle on NDVI, this index has being used in monitoring forests around the world. NDVI has been used in the study of green vegetation in a variety of biomes from arid zones (Olssaon et al., 2005; Atkinson et al., 2011) and to mountain region globally (Krishnaswami et al., 2013). With the development of geospatial technologies in the 21st century, new sensors with algorithms have been developed to remove certain disadvantages in NDVI. Enhanced Vegetation Index (EVI) was developed to improved sensitivity in high biomass regions and to reduce the effect of soil background noise and atmospheric influence (Huete et al., 2002; Matsushita et al., 2007). MODIS vegetation indices products (NDVI & EVI) have been used effectively for characterizing the vegetation condition process and biophysical/biochemical information (Busetto et al., 2008).

Over the years, the utility of Moderate Resolution Imaging Spectroradiometer (MODIS) datasets has increased tremendously in monitoring and detecting vegetation health, disturbance, logging and fires across large areas (Amiro et al., 2000; Epting et al., 2005). Spectral indices have been used to detect changes and measure vegetation vigour or biomass of the forest (Gillanders et al., 2008; Potter et al., 2012; De Jong et al., 2012). Many researchers have been interested in long-term ecosystem change studies to understand which factors are driving changes in an ecosystem at landscape scales (Sheng Pei et al., 2011).

The main objectives of this chapter are to document vegetation response and explore the possible role of climate variation in changes in NDVI/EVI over a 14-year (2001-14) period in the Nilgiri Biosphere Reserve and adjacent areas.

4.2. Materials and Methods

4.2.1. Materials

4.2.1.1. MODIS-NDVI &EVI dataset

MODIS (Moderate Resolution Imaging Spectro-radiometer) NDVI and EVI 16-day composite grid data, C5, MOD13A2 were downloaded from LPDAAC (Land Processing Distributed Active Archive Center, https://lpdaac.usgs.gov).MODIS tile no. h25v07 was download. A total of 322 time-series images were captured with 16-day interval from 2001 to 2014 and 23 images each year. These data was reprojected from Albers equal area projection to WGS84 UTM zone 43N from the original projection using the MODIS reprojection tool (MRT) and nearest neighbor resampling technique was employed. The MODIS standard VI products computed from atmospherically corrected bi-directional surface reflectance that have been masked for water, clouds, heavy aerosols, and cloud shadows and include two gridded vegetation indices (NDVI, EVI) were used for our study (Running et al., 1994; Justice et al., 1998; Huete et al., 2002). Quality control was applied to the entire time series where pixels with 0 and 1 were kept for continuing for further analysis. We then used Generalized Additive Models (GAMs) was estimate the parameter for smoothing time-series for fitting the data and to reduce the image noises from atmospheric clouds, particles and shadows data (Wood, 2006).

4.2.1.2. Land Surface Temperature (LST) Data

The MODIS/Terra Land Surface Temperature (LST) and Emissivity 8-Day L3 Global 1 km Grid SIN V006 was used for the study for the same time period of 14 year. Same MODIS tile no. h25v07 was downloaded from the downloaded from LPDAAC (Land Processing Distributed Active Archive Center, https://lpdaac.usgs.gov). Each pixel value in the MOD11A2 is a simple average of all the corresponding MOD11A1 LST pixels collected within the 8 day period in sinusoidal projection. Here, the digital numbers (DN) which was in Kelvin was converted to degree Celsius by using the following formula: Temperature = (DN * 0.02) - 273.15 ºC

4.2.1.3. Climate Hazards Group InfraRed Precipitation (CHIRPS) Data

Climate Hazards Group InfraRed Precipitation with Station data (CHIRPS) is a 30+ year of global rainfall dataset for on a monthly basis. Spanning 50°S-50°N (and all longitudes), starting in 1981 to near-present, CHIRPS incorporates 0.05°(5km) spatial resolution satellite imagery

with in-situ station data to create gridded rainfall time series for trend analysis and seasonal drought monitoring. This dataset was downloaded for a period of 14 years from ftp://ftp.chg.ucsb.edu/pub/org/chg /products/CHIRP/monthly / and extracted into tiff format. It was resampled to 1 km spatial resolution for further analysis with MODIS datasets.

4.2.2. Methods

4.2.2.1. Trend analysis

Trend analysis was used to determine the spatial characteristics of vegetation cover across large landscape. Change in vegetation cover over time was determined by fitting a regression trend line with one variable, where y=ax + b. Here, x is the year starting from 2001 to 2014 and y= is the annual mean of all data sets for each year. The rate of change is referred to as trend (De Jong et al., 2012). The slope of the regression indicates the type of trend at each pixel, positive values indicate the average annual increase in vegetation cover (NDVI from 2001 to 2014) and negative values the average decrease in vegetation cover. The same technique was followed to calculate the slope for EVI, LST and Rainfall.

4.2.2.2. The Multiple Regression Model

Multiple regressions are a statistical technique which allows predicting one variable on the basis of several other variables. Multiple regression focuses on the relationship between a dependent variable (Y) and one or more other independent variables (Xi). In this method, vegetation indices (NDVI & EVI) are treated as dependent variables and environmental parameters such as LST and Rainfall of the region are considered independent variables.

In general, the multiple regression equation of Y on X_1, X_2, …, X_k is given by: $Y = b_0 + b_1 X_1 + b_2 X_2 + \ldots\ldots + b_n X_{n..}$

4.2.2.3. Correlation analysis

Correlation is the commonly used to analyze the relationship two variables. The relationship between the annual mean NDVI & EVI with climatic variables for 2001 to 2014 were analyzed based on the correlation coefficients for NDVI-LST, NDVI-Rainfall, EVI-LST and EVI-Rainfall.

4.3. Results & Discussion

4.3.1. Spatial and temporal variation

The linear regression (or temporal trend) analysis was done for temporal datasets for the period 2001-2014. Figure 4.1.a illustrates the annual mean NDVI of 14 years extracted for a 50-hectare permanent plot established in deciduous forest at Mudumalai (Sukumar et al., 1992). Considering the inter-annual variation, NDVI responded with four peaks and three troughs. There was abrupt negative change in 2001 and then a slow increase up to 2006. Another fall in NDVI was recorded followed by a gradually increasing trend until 2011 before a sharp fall in 2013.

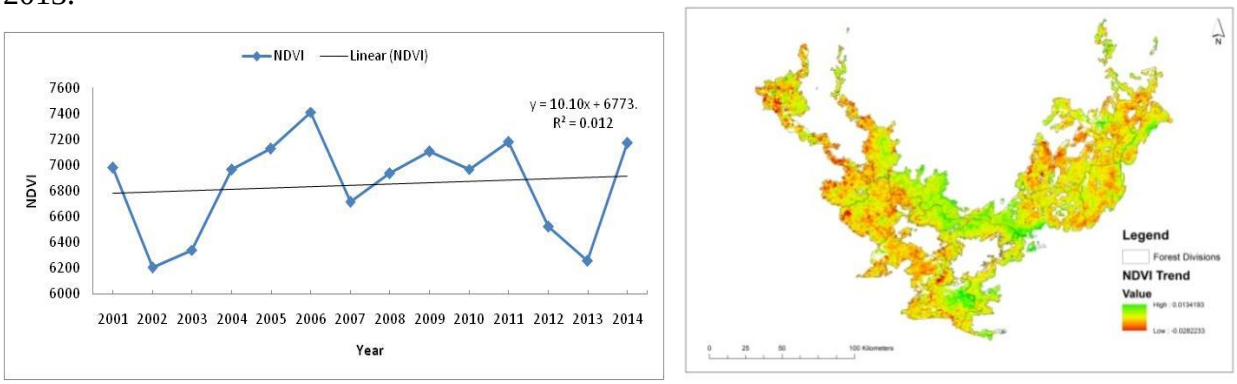

Figure 4.1: Inter-annual variability of annual NDVI (a) and trends of NDVI (b)

The NDVI trend values ranges from −0.0282 to 0.0134 which is shown in the figure 4.1.b. The spatial pattern of decreasing trend is shown from the northwest to the northeast direction. The distribution of NDVI trend varies in the landscape due to the heterogeneity of the land use and cover. A positive trend is found in regions with low elevation and slope which are characterized by agriculture, dry thorn and dry deciduous forest types. A decreasing trend is recorded in the wetter forest types and plantations.

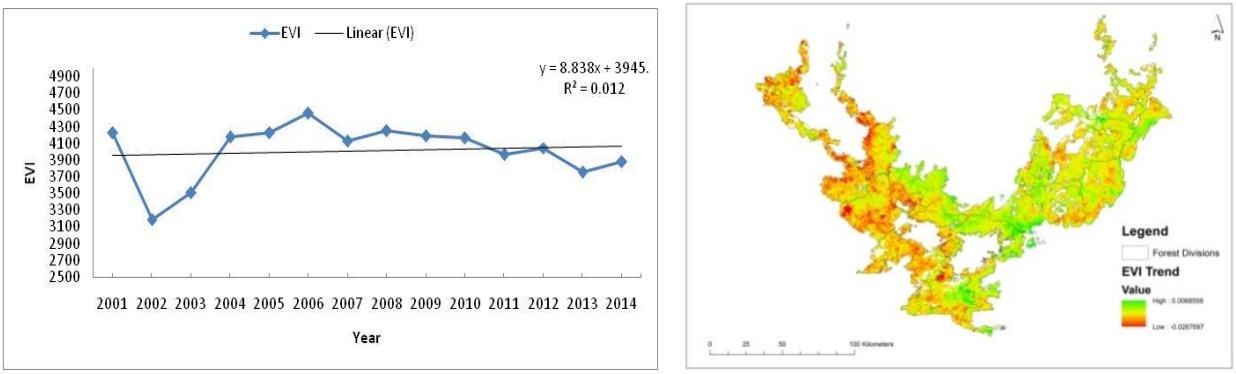

Figure 4.2: Inter-annual variability of annual EVI (a) and trends of EVI (b)

Figure 4.2.a illustrates the annual mean EVI of 14 years and it seems to be more stable as compared to NDVI over the same period. Here, the inter-decadal variation of the EVI responded differently with fewer peaks and troughs. EVI also showed abrupt decline in 2001 and then a

slow increases up to 2006, but then follows a gradually decrease up to 2011. The EVI trend values ranges from −0.0068 to 0.0267 which shows a similar spatial pattern of trend from the northwest to the northeast direction (Figure 4.2.b). The distribution of EVI trend is similar to the NDVI spatial pattern of trend with lesser intensity.

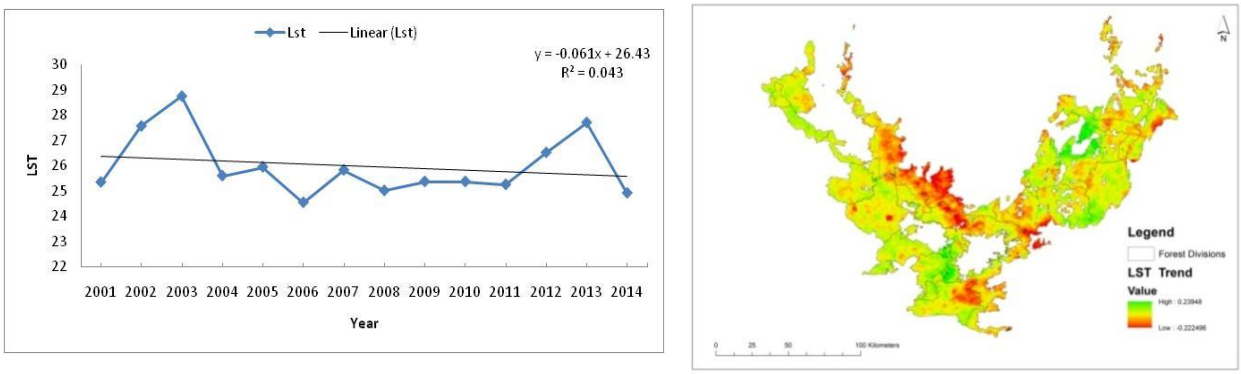

Figure 4.3: Inter-annual variability of annual LST (a) and trends of LST (b)

Figure 4.3.a illustrates the annual mean LST of 14 years. Considering the long-term inter-decadal variation, the LST responded differently with two peaks and three troughs. The LST trend values ranges from −0.2224 to 0.2394 shows a spatial pattern of decreasing trend from the northwest to the northeast direction (Figure 4.3.b). LST trend varies in the landscape due to the heterogeneity of the land use and cover. A negative trend is found in regions with low elevation and slope which are characterized by agriculture, dry thorn and dry deciduous forest types. This negative trend in LST seems related to the increase in biomass of invasive species in these areas, as well as possibly natural growth and succession of forests. A positive LST trend is seen in areas with wetter forest types and hilly areas.

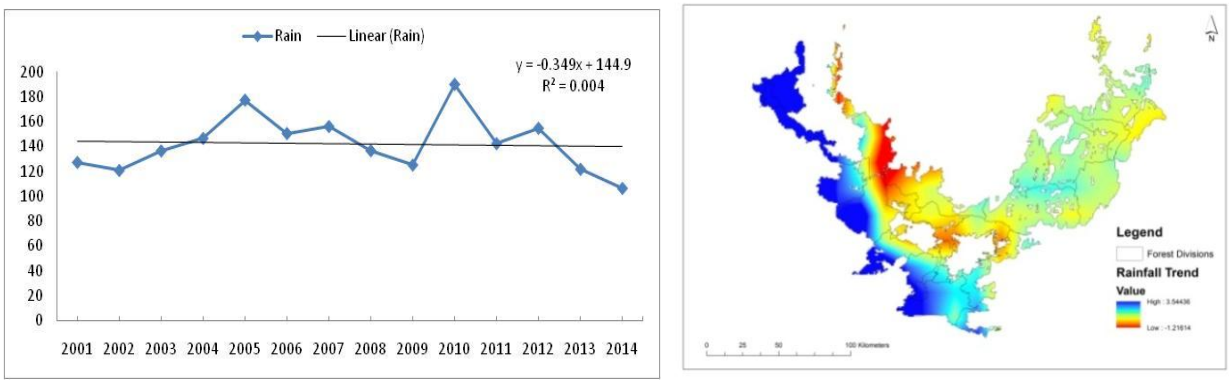

Figure 4.4: Inter-annual variability of annual rainfall (a) and trends of rainfall (b)

Figure 4.4a illustrates the annual rainfall over 14 years across the landscape. Notable deficits in rainfall are indicated during 2001-02, 2009 and 2014, while above normal rainfall was

experienced in 2005 and 2010. The spatial pattern of rainfall trend values ranges from −1.21 to 3.5 shows increasing trend in the western side and decreasing trend on the northwestern side (Figure 4.4.b). The distribution of rainfall tends to vary in the landscape due to the complex topographic heterogeneity. A negative trend is seen in the rain shadow areas with low elevation and slope characterized by dry thorn and dry deciduous forest types, whereas a slight positive trend is seen along the windward side and areas covered with moister forest types.

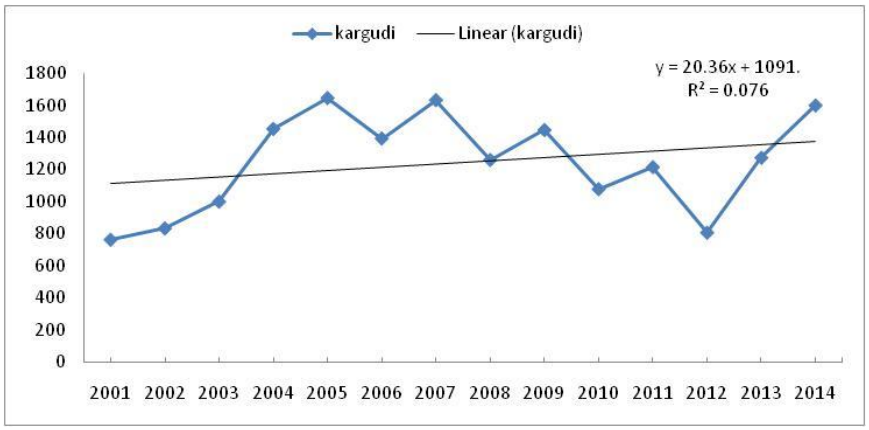

Figure 4.5: Inter-annual variability of rainfall measured at Kargudi

In Figure 4.5, rainfall from the ground station at Kargudi (Mudumalai), close to the 50-hectare forest plot mentioned earlier, is shown over the 14 year period. The overall drought of 2001-02 and the above normal rainfall of 2005, seen across the landscape, are captured here. However, there are differences in the subsequent years, emphasizing the importance of local variation in rainfall across complex landscapes.

4.3.2. The Multiple Regressions

For each pixel in the NBR raster layers, the following two regression models were fitted:

(a) NDVI ~ LST + rainfall
(b) EVI ~ LST + rainfall

The sample size for each model was 14, corresponding to a set of values for each year during the study period of 2001-2014. A regression coefficient was considered significant if its P-value was < 0.1. A statistically significant positive regression coefficient in a model indicates that the dependent variable (NDVI or EVI) tends to increase with the independent variable (LST or rainfall) under consideration, and vice versa.

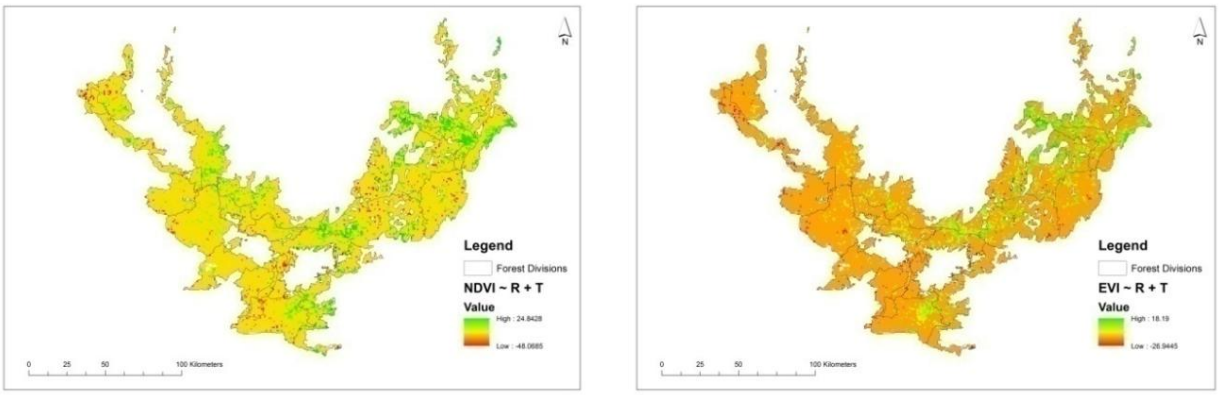

Figure 4.6: Regression slope parameter estimates for **(a)** NDVI and Rainfall **(b)** EVI and Rainfall

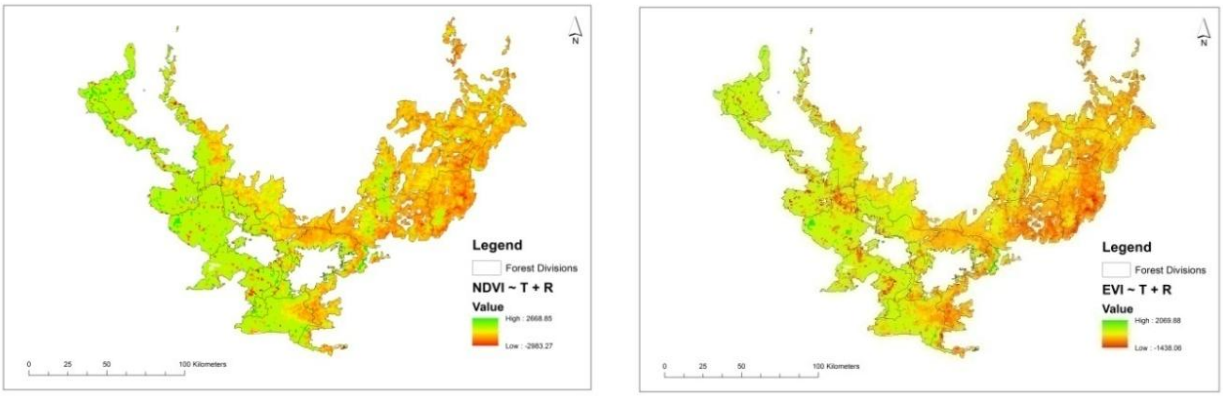

Figure 4.7: Regression slope parameter estimates for **(a)** NDVI and LST ***(b)*** EVI and LST

Figures 4.6 and 4.7 show the relationships between the vegetation indices and rainfall and LST, respectively. There appears to be considerable variation is the vegetation indices responses to these environmental factors, which may partly be due to spatial variation in topography, altitude, vegetation type and degree of anthropogenic disturbance. However, a few broad patterns are discernible:

i) Both vegetation indices appear to respond positively to increasing rainfall on the eastern part of NBR, while either responding negatively or showing no significant relationship to rainfall on the western part.

ii) Conversely, both vegetation indices appear to respond negatively to increasing LST on the eastern part of NBR and positively to increasing LST on the western part of NBR.

A possible interpretation of this result is that the vegetation is moisture limited in the eastern, drier part of NBR and temperature (energy) limited on the western, wetter part of NBR. Thus greenness (NDVI or EVI) on the eastern part of NBR would increase with increasing rainfall, but would decrease or remain the same with increasing temperature (which effectively increases moisture stress in an already moisture-limited system). Conversely, the greenness on the western part of NBR would increase with increasing LST, resulting from the positive effect of higher

energy availability for plant growth in a region that already has adequate moisture, while either not responding to, or decreasing, with increasing rainfall (the latter scenario could potentially be due to the negative effects of excessive water on plants, including water logging, which reduces the availability of oxygen to the roots).

An alternate interpretation of the relationship between the vegetation indices and LST is that LST is not the cause, but the consequence of the impact of vegetation on local microclimatic conditions. Because LST can both effect and be affected by vegetation, there remains the possibility of positive feedback loops. For instance, increases in LST can reduce vegetation cover, which can further increase LST, and vice versa. A similar positive feedback loop between rainfall and vegetation cover may also be possible, although it is unclear how strong such a feedback would be at the scale we considered. For instance, recent studies have suggested that monsoonal precipitation in parts of southwestern Kerala may have decreased in recent decades (Kumar et al., 2009; Rajendran et al., 2012; Devaraju et al., 2015; Roxy et al., 2015). We note that these relationships will also affected by the uncertainty in values of the environment variables, particularly rainfall. We did not incorporate this uncertainty in our models but doing so would modify both the slope estimates and corresponding P-values.

4.3.3. Spatial variance in vegetation with climate variables

The model comprising NDVI and LST has been applied for each pixel (2001-2014) and was also applied to evaluate the relationship between NDVI-Rainfall, EVI-LST and EVI-Rainfall. From the modeling, it was shows that the relationship between NDVI and the explanatory variable displays variability in the temperature due to rainfall gradient in the landscape. The intercept, slope and coefficient of R^2 parameters were calculated by the model between NDVI-LST which varied in the space over the study area.

We also model the lag effect of LST and rainfall for which it was applied to each pixel 13 years instead of 14 years. It was done to see the after affect of rain and temperature on the vegetation in long run. The lag effect of one year was tested for rainfall and temperature on vegetation.

In figure 4.8 the spatial patterns of NDVI-LST was estimated and mapped which appear to correspond to the distribution of vegetation and land cover. The intercept increases in value from the western to the eastern side. The slope decreases in the opposite direction while the coefficient of R^2 seems to displays higher values in the east than in the west of the study area. Where dry deciduous and dry thorn vegetation dominates are affect negatively by temperature. But NDVI LST lag results, the intercepts seems to be low in agricultural, plantation and in higher altitudes areas, dry deciduous and dry horn forested areas. The magnitude of the slope increases in the western side whereas decreases in the eastern side. The coefficient of R^2 seems to be lower with 15% of the entire area with few places in patches with high value

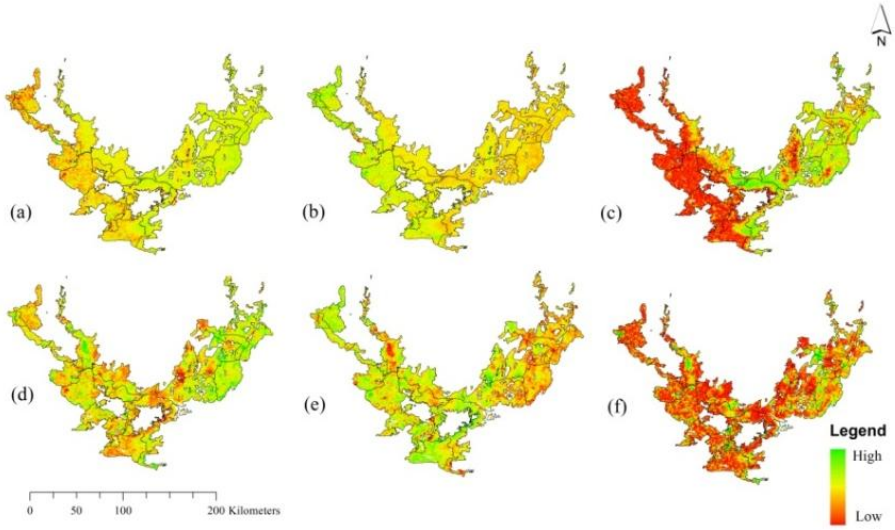

Figure 4.8: Summary results of the regression between NDVI-LST and NDVI-LST lag estimated from the mean values of the variables. The range of values for the figures can be seen in table 4.1.

Table 4.1: Summary of NDVI-LST and NDVI-LST lag (one year) correlation values.

	NDVI lst			NDVI lst lag		
	Intercept	Slope	R.squared	Intercept	Slope	R.squared
	a	b	c	d	e	f
High	75818.3	40062	1	56295	1668.2	1
low	-973049	-2806.97	0	-31903.5	-2092	0

.

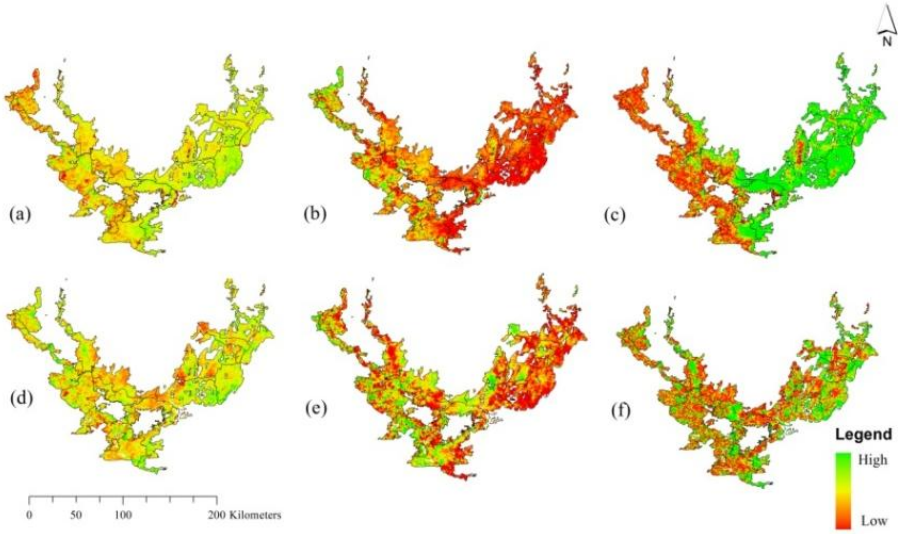

Figure 4.9: Summary results of the regression between EVI-LST and EVI-LST lag estimated from the mean values of the variables. The range of values for the figures can be seen in table 4.2.

Table 4.2: Summary of EVI-LST and EVI-LST lag correlation values

	EVI lst			EVI lst lag		
	Intercept	Slope	R.squared	Intercept	Slope	R.squared
	a	b	c	d	e	f
High	32362.4	108221.5	1	31605.7	1692.09	1
low	-260835	-1188.25	0	-35501.6	-1103.81	0

Figure 4.9 shows the spatial patterns of EVI-LST which were mapped and appear to correspond to the distribution of vegetation and land cover type. The slope of the relationship is strongly negative for the eastern drier part of the landscape dominated by dry deciduous and dry thorn vegetation. Thus, temperature seems to be negatively affecting the productivity of the vegetation in tropical dry forest. The EVI-LST lag results are more ambiguous.

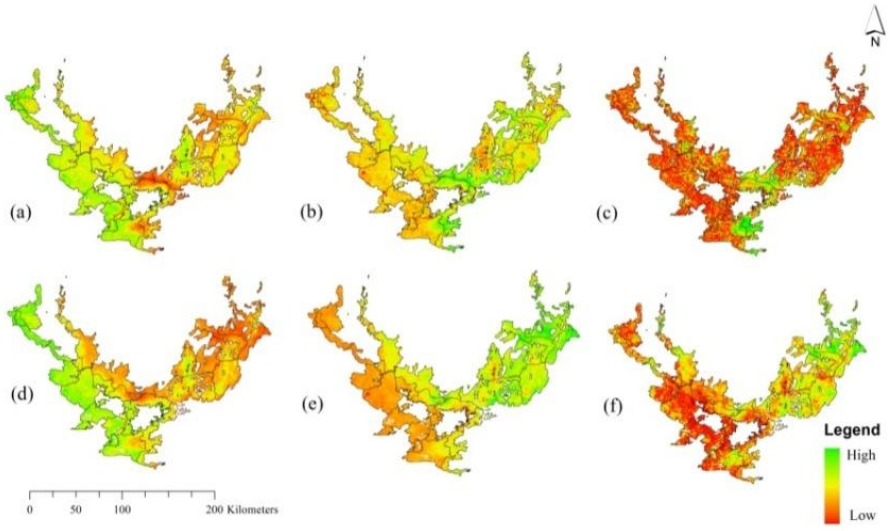

Figure 4.10: Summary results of the regression between NDVI-Rainfall and NDVI-Rainfall lag estimated from the mean values of the variables. The range of values for the figures can be seen in table 4.3.

Table 4.3: Summary of NDVI-Rainfall and NDVI-Rainfall lag correlation values

	NDVI Rainfall			NDVI Rainfall lag		
	Intercept	Slope	R.squared	Intercept	Slope	R.squared
	a	b	c	d	e	f
High	154581.5	314.0.17	1	11508.6	48.4276	1
low	-61501.9	-57.0033	0	-681.182	-96.743	0

Figure 4.10 shows the spatial patterns of NDVI-Rainfall relationship. The slope of the relationship is negative with time lag of one year in the drier eastern part of the landscape covered with dry deciduous and dry thorn forest. In the western wetter forested region the opposite relationship is seen, possibly as a result of diminished solar radiation during years with higher rainfall.

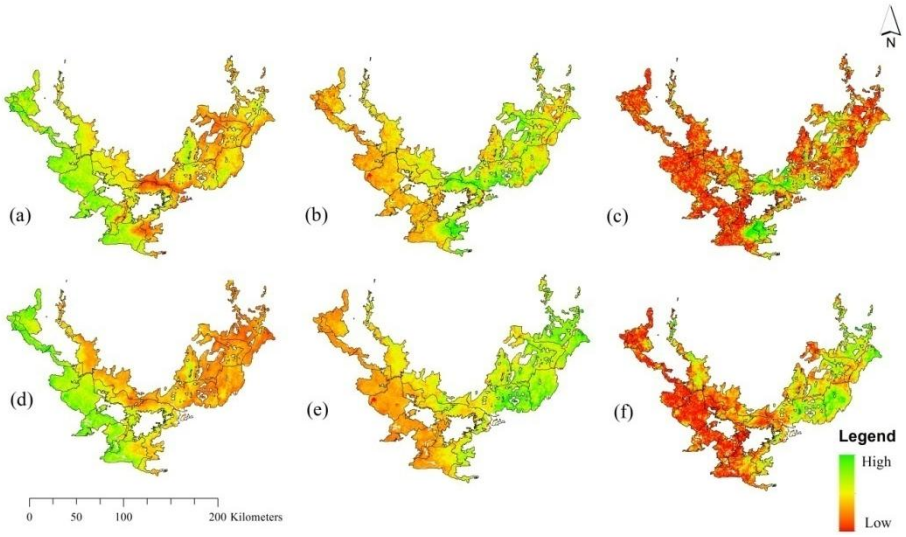

Figure 4.11: Summary results of the regression between EVI-Rainfall and EVI-Rainfall lag estimated from the mean values of the variables. The range of values for the figures can be seen in table 4.4.

Table 4.4: Summary of EVI-Rainfall and EVI-Rainfall lag correlation values

	EVI Rainfall			EVI Rainfall lag		
	Intercept	Slope	R.squared	Intercept	Slope	R.squared
	a	b	c	d	e	f
High	8103.63	84.8205	1	8550.6	37.501	1
low	-14612.9	-36.5748	0	-918.41	-59.9359	0

Figure 4.11 shows the spatial patterns of EVI-Rainfall relationship. The slope decreases from positive in the drier eastern side to negative in the wetter western side of the landscape. The coefficient of R^2 seems slightly stronger in the eastern part of the study area where dry deciduous and dry thorn vegetation dominates. In the case of EVI-Rainfall lag results, the slope is again positive on the eastern side and negative on the western side. The coefficient of R^2 values is also much higher in the eastern part. The patterns of EVI-Rainfall relationships without lag and with one year lag are thus similar, but the latter showing stronger statistical relationships.

4.3.4. Cross-validation of Correlation with the 50 hectare plot and Ground rainfall station

The annual mean values of variables (NDVI, EVI, precipitation, temperature and rainfall from the Kargudi ground station) for the period of 2001 to 2014 is extracted for the ROI (Region of interest i.e. 50 hectare plot) and shown in Table 4.5. Correlation analysis was done to have an understanding at the local scale of the plot as to how vegetation is responding with one year of lag effect of LST and rainfall.

Table 4.5: Extracted values of Mudumalai 50-hectare plot for 14 years

Year	NDVI	EVI	LST	CHIRPS Rainfall (cm)	Kargudi Rainfall (cm)
2001	6982.21	4228.54	25.34	127.21	76.37
2002	6206.74	3185.85	27.56	120.71	83.43
2003	6341.84	3508.99	28.75	136.45	100.17
2004	6966.21	4179.73	25.59	146.55	145.55
2005	7129.52	4224.44	25.94	177.49	164.8
2006	7412.76	4461.60	24.54	150.52	139.55
2007	6715.56	4123.66	25.82	156.14	163.48
2008	6938.20	4251.87	25.01	136.64	126.17
2009	7103.42	4188.49	25.36	125.09	144.85
2010	6970.13	4167.06	25.36	190.16	107.94
2011	7178.65	3963.91	25.25	142.34	121.7
2012	6520.28	4044.25	26.51	154.77	80.78
2013	6258.35	3755.78	27.71	121.68	127.53
2014	7169.99	3876.53	24.91	106.23	160.13

4.3.4.1. Relationship of vegetation without lag effect

The correlation between the annual mean NDVI & EVI and the climatic variables was tested for 14 years' data. A correlation of 0.226 and 0.447 was found respectively for NDVI versus rainfall and EVI versus rainfall, but using the data from the Kargudi weather station the strength of the correlation increased considerably. Considering the absolute value or the critical value of 0.25, pixels having the above value of 0.25 tend to increase in EVI with increasing rainfall but in case of the NDVI the correlation found to be below the critical value. In the case of NDVI-LST and EVI-LST the correlation was -0.903 and -0.796, respectively. Using the critical cut off of -0.25, the temperatures tend to have negative relationship with both NDVI and EVI, which means that greenness decreases with increase in temperature.

Table 4.6: Correlation values for ROI without lag effect

	NDVI	EVI	LST	C_Rain	K_Rain
NDVI	1.000				
EVI	0.783	1.000			
LST	**-0.903**	**-0.796**	1.000		
C_Rain	**0.226**	**0.447**	-0.170	1.000	
K_Rain	**0.499**	**0.398**	-0.403	0.097	1.000

4.3.4.2. Relationship of vegetation with lag effect

The correlation between the annually mean NDVI & EVI and the climatic variables was tested with one year lag. The analysis was done for 13 years with one year lag. A correlation of one year lag of **0.399** and **0.431** were found for NDVI-rainfall and EVI-rainfall, respectively with satellite data. However, the strength of the lag correlation doubles when data of Kargudi rainfall is used. Considering the absolute value or the critical value of 0.25, pixels having the above value of 0.25 tend to increase in EVI & NDVI with increased rainfall and one year lag. Considering the absolute value or the critical value of -0.25, pixels having values below –0.25 and seems that there is a weaker relationship between temperature and NDVI or EVI of the corresponding or preceding year as compared to rainfall.

Table 4.7: Correlation values for ROI with Lag effect

	NDVI	EVI	LST	C_Rain	K_Rain
NDVI	1.000				
EVI	0.782	1.000			
LST	**-0.010**	**-0.141**	1.000		
C_Rain	**0.399**	**0.431**	-0.329	1.000	
K_Rain	**0.729**	**0.837**	-0.350	0.296	1.000

4.4. Conclusions

The study examined the condition of vegetation using MODIS composite NDVI and EVI time series at 16-day intervals to monitor changes in greenness across the landscape during 2001-14. Across the landscape there seems to be overall greening in drier areas covered with dry deciduous and dry thorn forest. Browning is seen in the moist and evergreen forested regions and human-dominated areas of the landscape. The spatial pattern of greening of the eastern side and browning of the western side overall requires adequate explanation. The results of multiple regression model shows that rainfall has a positive effect but temperature tends to have negative effect on the vegetation. Vegetation responds to rainfall with a one-year lag positively. Using weather data from the ground station (Kargudi) seems to more strongly and realistically show relationships with NDVI & EVI.

The changes in vegetation in response to environmental factors requires further enquiry with temperature and rainfall data from long-term monitoring sites in the region. The study also showed that the relationship between NDVI & EVI and precipitation becomes stronger with a time-lag effect in the model. In future, a methodology can be developed to test the monthly lag between NDVI and precipitation as NDVI response to accumulated moisture, with higher spatial and temporal availability of the datasets with ground validation.

Chapter 5

Accessing the spatial pattern of stress using the spatio-temporal anomalies

5.1. Introduction

Drought stress in tropical forests of the world can have a serious impact on global carbon, water, and energy cycles (Mokhtari et al., 2011). Drought is a combined effect of precipitation and evapotranspiration in a particular area (Wilhite and Glantz, 1985). Such recurring weather events bring significant water shortages, reduction in soil moisture, economic losses and adverse effects on the life of the local people (Mokhtari et al., 2011). Prolonged drought affects both plant and animal life, though intensities may vary in different regions (Dracup et al., 1980). With predicted climate change, the extent of area under drought is expected to increase in the years to come, with adverse effects on agriculture and natural ecosystems (IPCC 2007; Mir et al., 2012).

Tropical forest ecosystems of the world would respond over both at short (physiological) and longer (ecological) timescales to drought. Both kinds of responses help in understanding and establishing a relationship between and feedback from forest-climate ecosystem. With little spatial information on soil properties and plant functional types, the response of tree species and communities to drought is poorly understood. Advances in satellite-derived measurements of ecosystem properties and processes now provide information for understanding the short- and long-term responses to drought (Lawley et al., 2016; Vicca et al., 2016). Normalized Difference Vegetation Index (NDVI) is one of the simplest, most efficient and commonly used indices and was first suggested by Tucker in 1979 for studying vegetation health and changes.

In 1999, NASA launch the Terra satellite platform with Moderate Resolution Imaging Spectroradiometer (MODIS) instrument on-board which initiated a new beginning for remote sensing of the Earth System. It senses the earth's surface in 36 spectral bands with three different spatial resolutions of 250m, 500 m and 1 km. MODIS products (such as NDVI and EVI) have been used effectively for characterizing different vegetation states and processes, and extracting biophysical information (Spruce et al. 2011) and forest disturbance over large regions (Waring et al., 2011). A photosynthetic activity and canopy variation of the vegetation is measured by the two commonly used vegetation indices i.e. NDVI (Normalised Difference Vegetation Index) and EVI (Enhanced Vegetation Index). EVI was developed to remove the disadvantages of NDVI, namely the effect of canopy background signal and atmospheric influences (Huete et al., 2002; Setiawan et al., 2013). Apart from this, NDVI index is not free from data error during the rainy season, saturation effects over dense vegetation areas, etc. Therefore, other parameters are needed to ensure more accuracy in interpreting green biomass changes over time. The variation may be related to the phenological response to radiation, steep slopes, reduces moisture and amount of vegetation (Goetz 1997). Studies done on at several spatial scales (25m to 1.2km)

indicate large changes in soil moisture and vegetation cover with rise in surface temperature rise. The ratio of LST/NDVI increases at the time of drought (Zhengming et al., 2004).In this study; we examine the spatial pattern of vegetation stress with standardised anomalies and impacts of drought on vegetation in the study area, as well as response of vegetation to regional climatic oscillations such as El Niño and La Niña.

5.2. Materials and Methods

All the datasets of chapter 4 were used for the same year of 14 years.

5.2. 1.Standardised anomaly

NDVI data acquisition and processing NDVI values were extracted. Then, NDVI means were calculated for each location and for each year. To characterize the temporal variation in vegetation index (VI) across the NBR, we calculated vegetation anomalies in terms of NDVI anomalies as the departure from the 2001-2014 mean ($NDVI_{2001-2014}$), normalized by the standard deviation (σ). NDVI surfaces were grouped annually to examine annual differences by computing the mean of images that correspond to each year. $NDVI_{anomaly}$ was calculated for each year on a pixel-by-pixel basis. Similar analysis was carried out using the MODIS EVI & LST and CHIRPS. Approaches for the analysis were done using the same methodology followed by Atkinson et al 2011. In addition, NDVI, EVI curves and amount of rainfall (mm) were plotted together to verify the correspondent variations. However, to investigate the relationship between NDVI, rainfall and for the entire study period (2001-2014 was used.

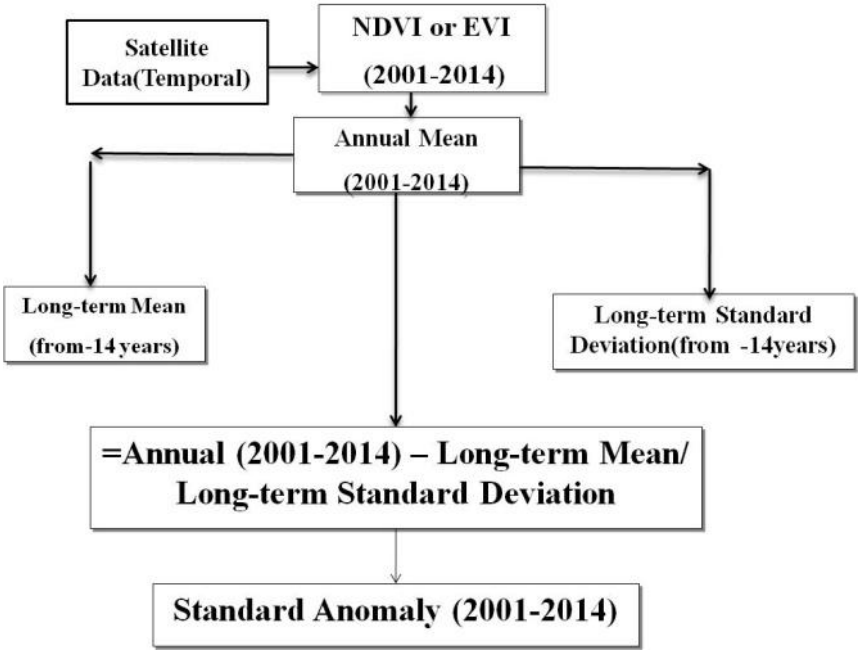

Figure 5.1: Methodology for Standardised Anomalies

5.3. Results and Discussion

5.3. 1.Temporal pattern of NDVI and EVI of Mudumalai 50 hectare Plot

The temporal patterns of vegetation change at the regional scale helps in understanding the interaction between environmental factors and natural ecosystems. The natural fluctuations in seasonal and annual mean value of NDVI & EVI during 2001-14 are used to evaluate the influence of climatic factors on vegetation. There is a higher degree of variation in NDVI values as compared to EVI values. Drought years such as 2001, 2002, and 2012 are captured in the low NDVI values during the dry season in the early part of the following year.

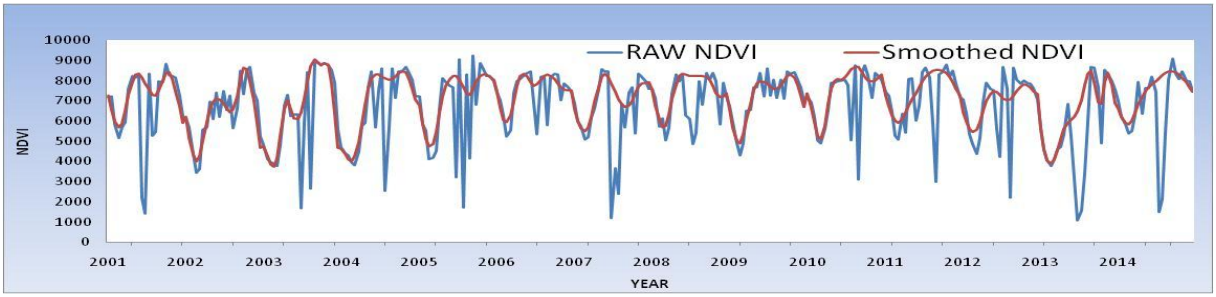

Figure 5.2: Time series of yearly raw NDVI (blue) and smoothed NDVI (red) data for the selected region of interest (Mudumalai 50 hectare Plot).

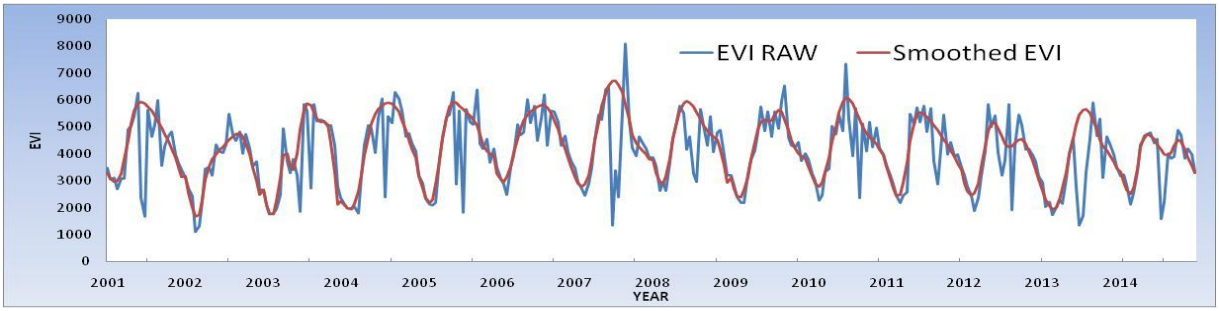

Figure 5.3: Time series of yearly raw EVI (blue) and smoothed EVI (red) data for the selected region of interest (Mudumalai 50-hectare Plot).

In order to understand the role of rainfall interannual variation during the vegetation growing season, anomalies were computed for each year from 2001 to 2014. In addition, NDVI curves and EVI curves were plotted to check the corresponding variations in vegetation responses. Further, to investigate the relationship between NDVI & EVI with rainfall and LST, these values were extracted for the selected region of interest (Mudumalai 50 hectare plot).

5.3. 2. NDVI and EVI temporal analysis

The NDVI & EVI patterns of annual variability of the 50 hectare plot during the period 2001–2014 are shown in Figure 5.4. Due to phenological change in the vegetation, the curves exhibit major peaks and troughs which coincide with the wet and dry seasons of the study area.

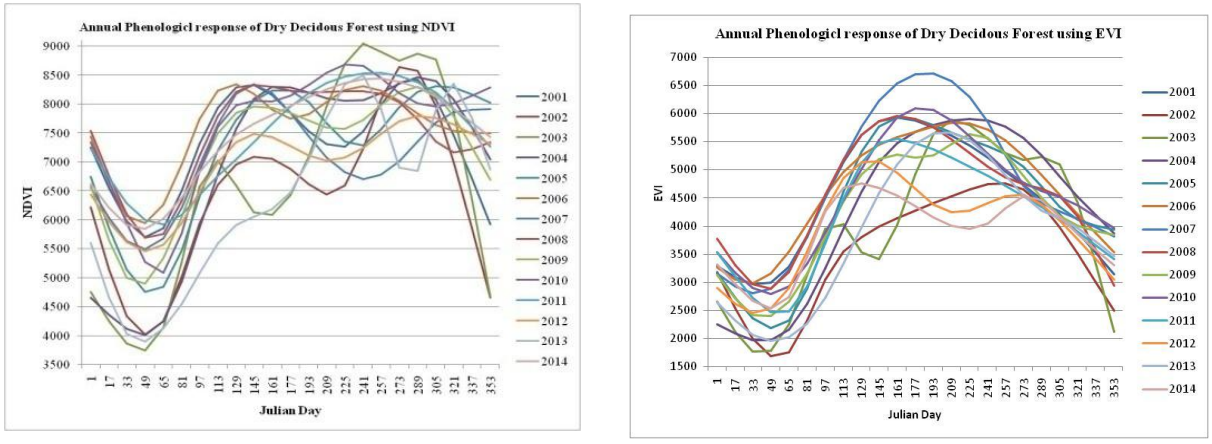

Figure 5.4: Annual mean values NDVI (left) and EVI (Right) for dry deciduous forest (50 hectare plot)

The peak periods of increased NDVI or EVI correspond to the rainy season, as expected, and the troughs with the dry season. Actually, the NDVI values correspond to three stages, an increasing greening stage with leaf flushing, a steady stage over several weeks in some years or a peak at the end of vegetation growth, and a declining stage with deciduousness or leaf shedding. As NDVI also capture moisture content the values remain high over an extended period in contrast to EVI that shows a clearer peak during the monsoon period followed by a decline. The inter-annual variations are modulated by the nature of rainfall spread in a particular year. The low NDVI and EVI values or slow responses correspond to years following drought (2002-03 and 2011-12) as shown in figure 5.4.

5.3.3. Relationship between annual EVI, NDVI and climate factors

The saturation effect over dense vegetation seen in mean NDVI is absent in EVI for conditions prevailing over the 50 hectare plot.

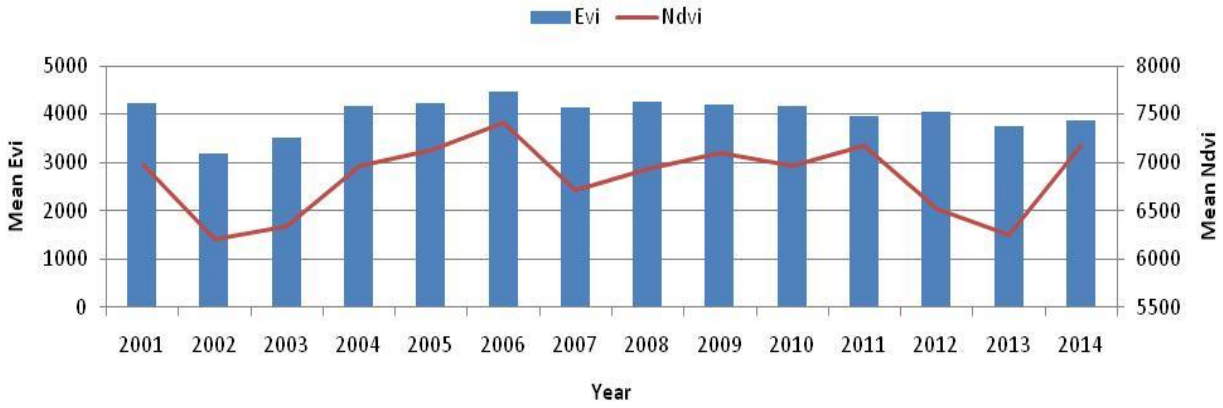

Figure 5.5: Annual Distribution of NDVI and EVI (2001-2014)

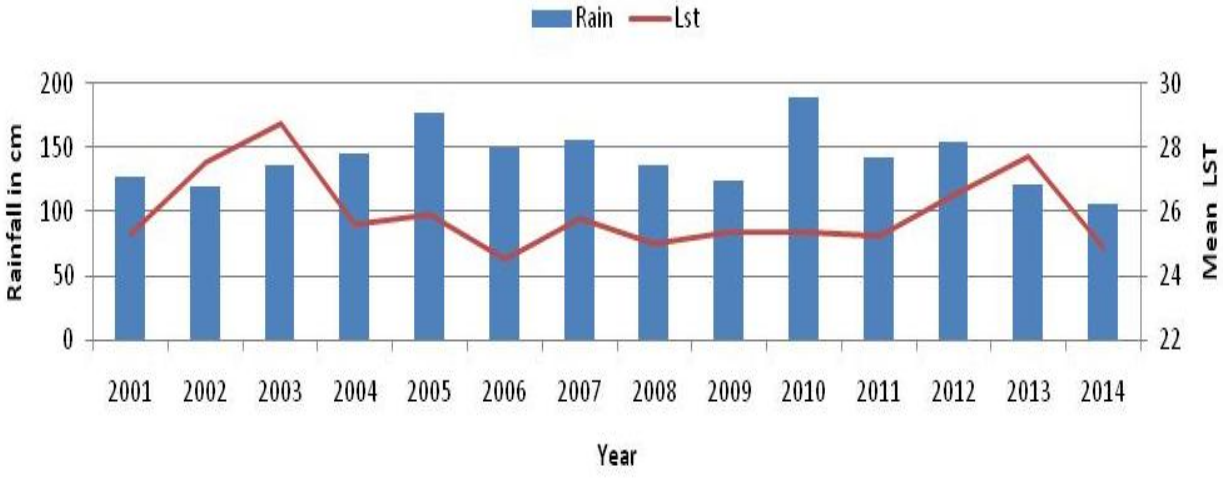

Figure 5.6: Annual Distribution of Rainfall and LST (2001-2014)

Figure 5.5 shows the annual pattern of mean NDVI and EVI. EVI was generally at a higher level throughout the period. NDVI seems more sensitive in capturing the influence of rainfall and temperature on the vegetation. On one other hand, rainfall (Figure 5.6) has a positive effect in 2006 and 2011 NDVI mean values which seem to follow the lag effects of rainfall, while the temperature effects exhibit a steady increase from 2001 till 2003 and from 2011 to 2013.

This is clearly illustrated in the NDVI and EVI values in 2002. The year 2003 and 2013 marked the extreme affect of El Nino years, while the NDVI and EVI values of 2005 and 2006 marked the extreme affect of La Nina years. It was seen that the plot had been affected by the extremes events of wet climate conditions and the dry climate conditions profoundly affected vegetation dynamics of the region. This result could indicate that the changes in the NDVI and EVI variations can explain vegetation dynamics with extreme La Niña year (2005, 2010) and extreme El Niño years (2002).

5.3. 4. Annual Vegetation Anomalies of NDVI and EVI

We also used MODIS time series satellite datasets of vegetation indices to map the spatial pattern of vegetation stress. NDVI and EVI anomalies show a relationship with drought years and the occurrence of fire. While increased vegetation stress in the drier forest types was seen during 2002-03, the stress shifted to the more moist western side after 2006.

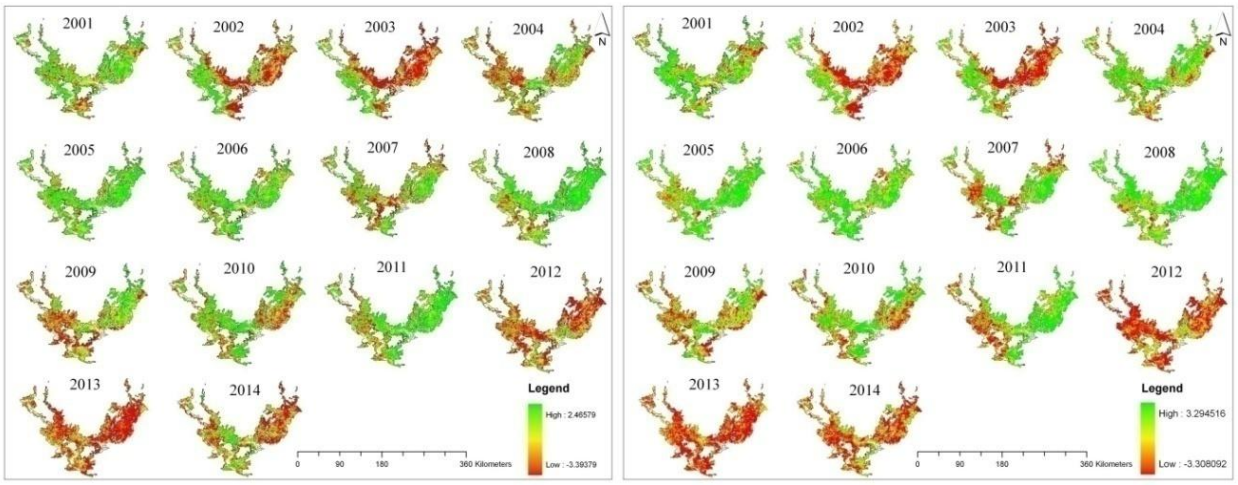

Figure 5.7: NDVI Annual anomaly (top-left) and EVI Annual anomaly (top-right).

Annual NDVI and EVI anomaly analyses indicated that several areas during the years 2001, 2002, 2003, 2007 , 2009, 2012, 2013 and 2014 experienced vegetation stress (> 1σ) in relation to the 2001-2014 mean. Preliminary results indicate changes in vegetation cover detected from the NDVI and EVI annual means compared to the base year 2001.

5.3. 5. Annual climatic anomalies of LST and Rainfall

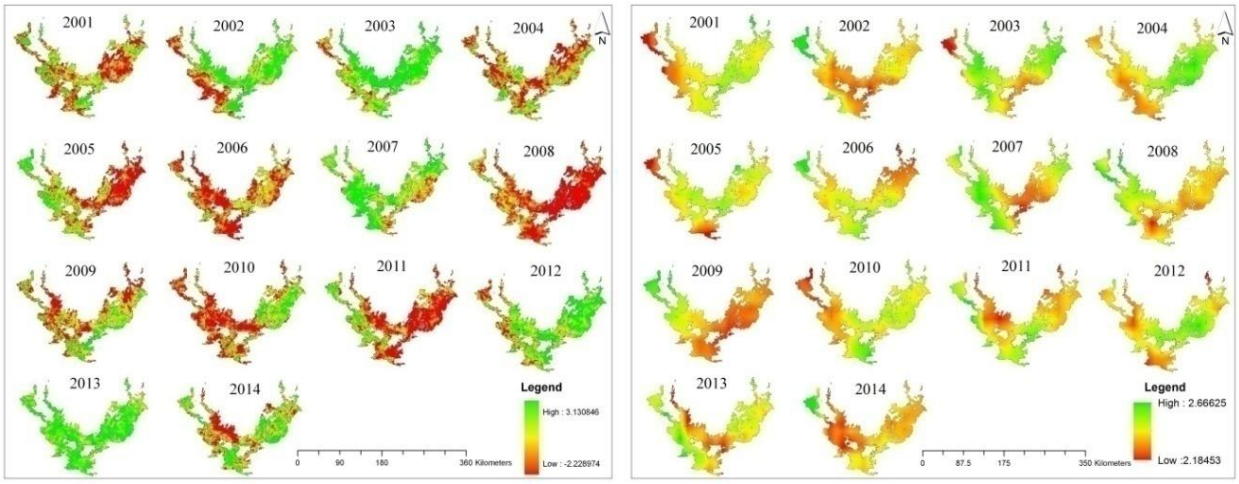

Figure 5.8: LST annual anomaly (top-left) and Rainfall annual anomaly (top-right).

We also used MODIS and CHIRPS time series satellite datasets of land surface temperature and rainfall to map the spatial pattern of stress in moisture. LST and Rainfall anomalies show a relationship with drought years and the occurrence of fire. While increased LST stress in the drier forest types was seen during 2002-03, in 2004 and 2005 stress shifted to the more moist western side and in 2006 and 2009 on the eastern side. Annual LST anomaly analyses indicated that several grids during the years 2001, 2002, 2003, 2007 , 2009, 2012, 2013 and 2014 experienced LST stress (> 1σ) in relation to the 2001-2014 mean. The changes in NDVI and EVI anomalies in vegetation cover detected seem to follow the effect of LST in the same year.

The negative rainfall anomalies of 2002, which covered the entire NBR, seemed to affect the forest for a long period (about 4 years) and from which the region recovered only in 2005. Positive anomalies took place in 2005 and 2010. Despite the stress with LST in 2007, the vegetation did not respond in 2007 with respect to NDVI and EVI. The rainfall stress of 2004 was reflected in the NDVI but not in the EVI. Rainfall Standardised anomalies provided insights into patterns of rainfall with stress mainly at the landscape level after 2010 and with the eastern side experiencing the long term drought effects which is shown by the NDVI and EVI vegetation anomalies.

5.3. 6. Annual dispersion of Mean and standard deviation in anomalies

The mean and standard deviation of NDVI, EVI, temperature, and precipitation for the study area were plotted along a 14 year time series to show that the mean and standard deviation values changed from one year to another. The general pattern of NDVI and EVI responds to the pattern of temperature well in the same year but with precipitation from previous years.

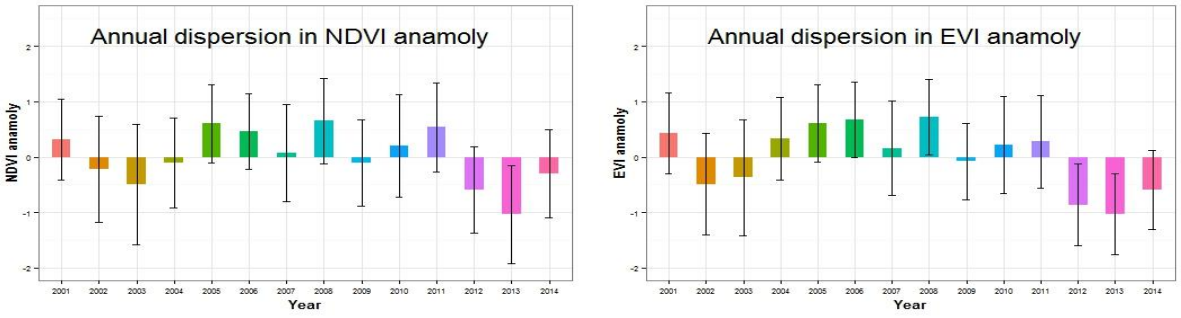

Figure 5.9: Annual dispersion of Mean and standard deviation in NDVI anomalies (top-left) and Annual dispersion of Mean and standard deviation in EVI anomalies (top-right)

Positive mean NDVI anomalies occurred in 2005, 2006, 2008 and 2010, and negative mean NDVI anomalies during 2002-04 which were drought years with similar conditions to the later part of the study during 2012-14. Similar conditions are found in EVI anomalies. The standard

deviation of the anomalies showed that the NDVI and EVI seemed to have high variability with negative variation in NDVI in 2013, but EVI captured negative variation for 2012 and 2013.

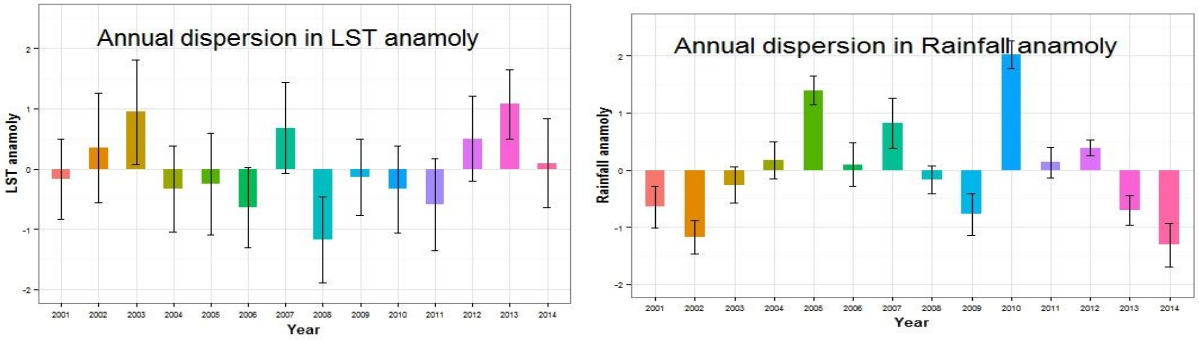

Figure 5.10: Annual dispersion of mean and standard deviation in LST anomalies (top-left) and Annual dispersion of mean and standard deviation in Rainfall anomalies (top-right)

However, the mean anomalies in LST were strongly positive in 2003, 2007 and 2013. The anomalies in rainfall were distinctively negative during 2001, 2002, 2009, 2013, and 2014, and positive during 2005, 2007, and 2010. This variability may differ with respect to particular land use and land cover types. Thus, simple mean of anomalies in a vegetation index for such a large area may not be an appropriate representation of the data, and therefore alternatives need further evaluation.

5.4. Conclusions

This study assesses vegetation stress across a large complex landscape, through integrating climatic and remote sensing data over time. NDVI and EVI curves were able to differentiate vegetation responses to rainfall. While the NDVI index integrates rainfall, temperature and soil water holding capacity, while EVI ignore soil moisture. NDVI and EVI anomalies show a clear relationship with drought years and the occurrence of fire. The LST and rainfall anomalies are dependent at the time when they occur. While increased vegetation stress in the drier forest types was seen during 2002-03, the stress shifted to the more moist western side after 2006. Prolonged stress was found in two periods i.e. 2002-2004 and 2012-2014 in the vegetation, with LST and rainfall anomalies being the reason behind this. The magnitude of this stress can be related to drought which is consider as climatic episodes and global climatic oscillations like the El Niño years affects the vegetation vigour negatively and La Niño positively.

Chapter 6

CONCLUSIONS

The Nilgiri Biosphere Reserve and adjoining regions have diverse vegetation across elevation and rainfall gradients, making it a complex system to study. In this study, land use and land cover changes in the Nilgiri Biosphere Reserve (NBR) and the broader landscape were studied using different remote sensing change detection techniques. Land-use/land cover classification was carried out using Landsat MSS (1973) and TM (1992), and IRS LISS3 (2011) data and an updated map was prepared for the study area. To assess the spatial and temporal patterns of the NBR landscape disturbances, we used linear spectral unmixing and change vector analysis techniques on multi-temporal remote sensing datasets. Major LU/LC changes have taken place in the area under plantations of tea and coffee, settlement and water bodies. There was an increase in forest regeneration (increase in biomass) during 1973-92, while a decline in vegetation fraction (decrease in biomass) and increase in soil fraction (degradation) during 1992-2011 was observed. Ground truth surveys indicate that the increasing trend in biomass in the drier areas could be due in part to increasing abundance of the invasive species *Lantana camara*, but also the high rate of regeneration of forest could have increased greenness in several protected areas. Negative trends are found in grassland/shola forest and evergreen regions while the positive trends are mainly spread across the primary moist and dry deciduous forests, and the tree savanna to grassland in the dry zone.

MODIS VI signal trend analyses indicate vegetation greening on the eastern side, when compared to the western side that was experiencing a browning trend between 2001 and 2014. Vegetation trends during this period, as recorded in vegetation indices (NDVI & EVI), were correlated with climatic parameters such as Land Surface Temperature and Rainfall of the region obtained from satellite-based records. Rainfall seems to have a positive effect on the vegetation with a lag of one year, while temperature tends to have a negative effect. The association of vegetation indices with LST seems to be significant but with rainfall was not. However, biomass from a permanent forest plot in the NBR was significantly correlated to rainfall data from a nearby weather station. NDVI and EVI anomalies also show clear relationships with drought years.

6.1. Deliverables

This project aimed at creating a baseline land cover/land use map of the Nilgiri Biosphere Reserve, a biodiversity hotspot. We were able to produce the high-resolution (24 m pixel) land cover maps using IRS LISS III imagery. We were also able to generate spatially explicit maps of forest degradation using multi-temporal series of high-resolution satellite data. We quantified forest degradation by using change detection techniques like change vector analyses, spectral mixture analysis and land use/land cover mapping for different time periods (1973-2011). Some

data were collected from the field to assesses aboveground biomass changes which can be useful for REDD inventories and important as a climate change mitigation mechanism (IPCC 2014). Two new objectives were added and successful results obtained. Work on time series analysis revealed interesting spatial-temporal trends for datasets used and correlations with lag effect between vegetation indices (NDVI & EVI) and climate variables (temperature & precipitation) using multivariate statistics and time-series analyses. The results have been validated with ground weather station and field data, which further bolsters the value of this work. This project involved statistical, geo-spatial and climate data analyses, as well as field work. We further investigated the linkages between drought and forest degradation patterns and global climatic oscillations like the El Niño and La Niña.

6.2. Future Directions

Global warming has could have played a role in significant vegetation changes in the NBR in recent years and it is susceptible to future climate change. However, assessing the causes and consequence of these spatio-temporal patterns will require new monitoring and analytical tools. Some of the limitations of this study is that only mean was considered for the data analysis. The maximum, minimum, and growing season may be more closely related with vegetation. More ground data from rainfall stations and forest plots should be used to establish correlations with the vegetation and climatic condition in the ground. Future research should focus on the use of higher spatial and temporal resolution datasets from to study the phenological cycle of vegetation with rainfall and other climate data. Land use modelling techniques for quantifying land use/land cover changes for future prediction should be carried out linking field-oriented research in understanding climate change its influence on vegetation dynamics and trends will have socio-economic implications and the future of the regional environment in the long run.

Chapter 7

References:

1. Adams, J.B., Smith, M.O. and Johnson, P.E. (1986) Spectral mixture modeling: a new analysis of rock and soil types at the Viking Lander I Site. *Journal of Geophysicical Research* 91: 8098-8112.
2. Agrawal, Arun., Daniel, Nepstad. and Ashwini, Chhatre. (2011) Reducing Emissions from Deforestation and Forest Degradation. *Annual Review of Environment and Resources* 36: 373–96.
3. Al-Bakri, Jawad Taleb., Salahat ,Mohammad., Suleiman, Ayman., Suifan, Marwan., Hamdan, Mohammad R.., Khresat, Saeb and Kandakji, Tarek (2013) Impact of Climate and Land Use Changes on Water and Food Security in Jordan: Implications for Transcending The Tragedy of the Commons. *Sustainability*, 5: 724-748.
4. Al-doski, Jwan., Mansor, S.B. and Shafri, H.Z.M. (2013) Change Detection Process and Techniques. *Civil and Environmental Research*. 3: 37- 45.
5. Amiro, B. D., Chen, J. M. and Liu, J. (2000) net primary productivity following forest fire for Canadian Ecoregions. *Canadian Journal of Forest Research* 30: 939-947.
6. Aragão, L.E.O.C., Malhi, Y., Roman-Cuesta, R. M., Saatchi, S., Anderson, L.O., Shimabukuro, Y.E. (2007) Spatial patterns and fire response of recent Amazonian droughts. *Geophysical Research Letters* 34: L07701.
7. Asner, G. P. (2009) Automated mapping of tropical deforestation and forest degradation: CLASlite. *Journal of Applied Remote Sensing* 3: 033543.
8. Atkinson, P.M., Dash, J. and Jeganathan, C. (2011) Amazon vegetation greenness as measured by satellite sensors over the last decade. *Journal of Geophysical Research Letters* 38: L19105.
9. Bannari, A., Morin, D., Huette, A.R. and Bonn, F. (1995) A review of vegetation indices. *Remote Sensing Reviews* .13: 95-120.
10. Busetto, L., Meroni, M. and Colombo, R.(2008) Combining medium and coarse spatial resolution satellite data to improve the estimation of sub-pixel NDVI time series. *Remote Sensing of Environment* 112: 118–131.
11. Champion, H.G. and Seth, S.K. (1968) A revised survey of forest types of India. GoI. New Delhi.
12. Chen, Jin., Gong, Peng., He, Chunyang., Pu, Ruiliang. and Shi, Peijun. (2003) Land-Use / Land-Cover Change Detection Using Improved Change-Vector Analysis, *Photogrammetric Engineering & Remote Sensing* 69: 369–379.
13. Cheng, C., Gamon, J.A., Fuentes, D.A., Mao, Z. Sims, D.A., Qiu, H,, Claudio, H,, Huete, A. and Rahman, A.F. (2006) A multi-scale analysis of dynamic optical signals in a Southern California chaparral ecosystem: a comparison of field, AVIRIS and MODIS data. *Remote Sensing Environment* 103: 369-378.

14. Choudhury, B. J. (1987) Relationships between vegetation indices, radiation absorption, and net photosynthesis evaluated by a sensitivity analysis. *Remote Sensing Environment* 22: 209–233.
15. Chuvieco, E., Ventura, G., Martin, M.P., Gomez, I. (2005) Assessment of multi temporal compositing techniques of MODIS and AVHRR images for burned land mapping. *Remote Sensing Environment* 94: 450-462.
16. Congalton, K. and Green, A. (1999) Assessing the accuracy of Remotely Sensed Data: Principles and Practices, New York. Lewis Publisher.
17. *Coppin,* P., *Jonckheere,* I., *Nackaerts, K., Muys, B., Lambin, E*. (2004) Digital change detection methods in ecosystem monitoring: a review. *International Journal of Remote Sensing* 25: 1565-1596.
18. Cuba, N., Marco, M., Rogan, J., Christman, Z., Williams, A., Schneider, L. C., and Lawrence, D. (2013) Modelling dry season deciduousness in Mexican Yucatán forest using MODIS EVI data (2000 – 2011). GIScience & Remote Sensing 50: 26–49.
19. Das, A., Krishnaswamy, J., Bawa. K.S., Kiran, M.C., Srinivas, V., Kumar, N.S., and Karanth, K.U. (2006) Prioritization of conservation areas in the Western Ghats, India. *Biological Conservation* 133: 16-31.
20. Dawelbait, M.A..A., and Morari, Francesco. (2011) LANDSAT, Spectral Mixture Analysis and Change Vector Analysis to Monitor Land Cover Degradation in a Savanna Region in Sudan (1987-1999-2008). *International Journal of Water Resources and Arid Environments* 1: 366-377.
21. De Jong, R., Verbosely, J., Schaepman, M. E. and de Bruin, S. (2012) Trend changes in global greening and browning: contribution of short-term trends to longer-term change. *Global Change Biology* 18: 642–655.
22. Dengsheng, L. (2006) The potential and challenge of remote sensing-based biomass estimation. International Journal of Remote Sensing 27: 1297–1328.
23. Devaraju, N., Bala, G., Modak, A. (2015) Effects of large-scale deforestation on precipitation in the monsoon regions: Remote versus local effects. *Proceedings of the National Academy of Sciences* 112: 257-3262.
24. Dracup, J.A., Lee, K.S. and Paulson, E.G. Jr. (1980) On the Definition of Droughts. *Water Resources Research* 16 : 297–302.
25. Dukes, J. S. and Mooney, H.A. (199) Does global change increase the success of biological invaders? *TREE* 14: 135-139.
26. Dutta, K., Reddy, C.S., Sharma, S. and Jha, C.S. (2016) Quantification and monitoring of forest cover changes in Agasthyamalai Biosphere Reserve, Western Ghats, India (1920-2012). *Current Science 110*, 508–520.
27. Elmore, A.J., Mustard, J.F., Manning, S.J. and Lobell, D.B. (2000) Quantifying Vegetation Change in Semiarid Environments:Precision and Accuracy of Spectral Mixture Analysis and the Normalized Difference Vegetation Index. *Remote Sensing of Environment* 73: 87-102.

28. Enkhzaya, Tsevengee and Tateishi, Ryutaro (2011) Use of phenological features to identify cultivated areas in Asia. *International Journal of Environmental Studies* 68: 9–24
29. Epting, J. and Verbyla, D. L. (2005) Landscape Level Interactions of Pre-Fire Vegetation, Burn Severity, and Post-Fire Vegetation over a 16-Year Period in Interior Alaska. *Canadian Journal of Forest Research* 35: 1367-1377.
30. Food and Agriculture Organization. (2013) Advancing agroforestry on the policy agenda: a guide for decision-makers. Buttoud G, Ajayi O, Detlefsen G, Place F, Torquebiau E. Agroforestry Working Paper no. 1. Rome: Food and Agriculture Organization of the United Nations.
31. Foody, G. M. (2002) Status of Land Cover Classification Accuracy Assessment." Remote Sensing of Environment 80: 185–201.
32. Franklin, S.E. (2001) Remote sensing *for* sustainable forest management. CRC Press LLC, Boca Raton, Florida, USA, 48pp.
33. Gillanders, S.N., Coops, N.C., Wulder, M.A., Gergel, S.E., Nelson, T. (2008) Multitemporal remote sensing of landscape dynamics and pattern change, describing natural and anthropogenic trends. *Progress in Physical Geography* 32: 503–528.
34. Goetz, S. J., (1997) Multi-sensor analysis of NDVI, surface temperature and biophysical variables at a mixed grassland site. International Journal of Remote Sensing. 18: 71–94.
35. Haines, Y.R. (2009) Land use and biodiversity relationships. *Land use policy* 26: S178-S186.
36. Halim, M.A., Shahid, A., Chowdhury, M.S.H., Nahar, M.N., Sohel, M.S.I., Nuruddin, M. J., and Koike, M. (2008) Evaluation of land-use pattern change in West Bhanugach Reserved Forest, Bangladesh, using remote sensing and GIS techniques. *Journal of Forestry Research* 19: 193–198.
37. Hall, F.G., Strebel, D.E., Nickeson, J.E., Goetz, S.J. (1991) Radiometric rectification: toward a common radiometric response among multidate, multisensor images. *Remote Sensing of Environment* 35: 11-27.
38. Hansen, M. C., Potapov Moore, P.V., R., Hancher M., Turubanova S. A., Tyukavina, A., Thau D., Stehman S.V., Goetz, S.J., Loveland, T. R., Kommareddy,A., Egorov, A., Chini, L., Justice, C.O. and Townshend, J.R.G. (2013) High-Resolution Global Maps of 21st-Century Forest Cover Change. *Science* 342: 850-853.
39. Herrmann, S. M., Anyamba, A. and Tucker, C.J. (2005) Recent trends in vegetation dynamics in the African Sahel and their relationship to climate. *Global Environmental Change* 15: 394-404.
40. Hiremath, A.J. and Sundaram, B. (2005) The Fire-Lantana cycle hypothesis in Indian forests. *Conservation and Society* 3: 26–42.
41. Houet, T., Verburg, P.H. & Loveland, T.R. (2010) Monitoring and modelling landscape dynamics. *Landscape Ecology* 25: 163-167

42. Huete, A., Didan, K., Miura, T., Rodriguez, E.P., Gao, X., and Ferreira, L.G., (2002) Overview of the radiometric and biophysical performance of the MODIS vegetation indices. *Remote Sensing of Environment* 83: 195–213.
43. IPCC. (2014) 2013 Supplement to the 2006 IPCC Guidelines for National Greenhouse Gas Inventories: Wetlands.
44. Jansen, L.J.M. and Di, G.A. (2002) Parametric land cover and land-use classification as tools for environmental change detection. *Agriculture, Ecosystems and Environment* 91: 89–100
45. Jeganathan, C., Dash, J. and Atkinson, P.M. (2010) Characterising the spatial pattern of phenology for the tropical vegetation of India using multi-temporal MERIS chlorophyll data. *Landscape Ecology* 25: 1125.
46. Jha, C.S., Dutta, C.B.S. and Bawa, K.S. (2000) Deforestation and land-use changes in Western Ghats, India. *Current Science* 79: 231-237.
47. Justice, D. H., Salomonson, V., Privette, J., Riggs, G., Strahler, A., Lucht, R., Myneni, R., Knjazihhin, Y., Running, S., Nemani, R., Vermote, E., Townshend, J., Defries, R., Roy, D., Wan, Z., Huete, A., van Leeuwen, R., Wolfe, R., Giglio, L., Muller, J.-P., Lewis, P., and Barnsley, M. (1998) The Moderate Resolution Imaging Spectroradiometer (MODIS): land remote sensing for global change research. *IEEE Trans-actions on Geoscience and Remote Sensing* 36: 1228–1249.
48. Khiry, M.A., (2007) Spectral Mixture Analysis for Monitoring and Mapping Desertification Processes in Semi-arid Areas, first ed. Rhombos-Verlag, Berlin.
49. Kodandapani, N., Cochrane, M. A., and Sukumar, R. (2004) Conservation threat of increasing fire frequencies in the Western Ghats, India. *Conservation Biology* 18:1553-1561.
50. Kodandapani, N., Murthy, I. K., Suresh, H. S., Dattaraja, H. S., Ravindranath, N. H., and Sukumar, R. (2001) Non timber forest product extraction, utilization and valuation: a case study from the Nilgiri Biosphere Reserve. *Economic botany* 55: 528–538.
51. Kodandapani, Narendran., Cochrane, M.A. and Sukumar, R. (2008) A comparative analysis of spatial, temporal, and ecological characteristics of forest fires in seasonally dry tropical ecosystems in the Western Ghats, India. *Forest Ecology and Management* 256: 607–617.
52. Krishnakumar, K.N., Prasada Rao, G.S.L.H.V. and Gopakumar, C.S. (2009) Rainfall trends in twentieth century over Kerala, India. *Atmospheric Environment* 43: 1940–1944.
53. Krishnaswamy, Jagdish., Robert, John. and Shijo, Joseph. (2014) Consistent response of vegetation dynamics to recent climate change in tropical mountain regions. *Global Change Biology* 20: 203-215.
54. Kurz, W.A., Dymond, C.C., Stinson, G., Rampley, G.J., Neilson, E.T., Carroll, A.L., Ebata, T. and Safranyik, L. (2008) Mountain pine beetle and forest carbon feedback to climate change. *Nature* 452: 987-990.

55. Kuzera, K., Rogan, J. and Eastman, J.R. (2005) Monitoring vegetation regeneration and deforestation using change vector analysis: MT. ST. Helens study area, in: ASPR 2005 Annual Conference. Baltimore, Maryland.
56. Lambin, E. F. and Strahler, A. H. (1994) Change-Vector Analysis in multi-temporal space: A tool to detect and categorize land-cover change processes using high temporal-resolution satellite data *Remote Sensing of Environment* 48: 231-244.
57. Laurance, W.F. (2007) Forest destruction in tropical Asia. *Current Science* 93: 1544-1550.
58. Lawley,V., Lewis,M., Clarke, K. and Ostendorf, B. (2016) Site-based and remote sensing methods for monitoring indicators of vegetation condition: An Australian review. *Ecological Indicators* 60: 1273–1283
59. Lepers, E., Lamin, E.F., Janetos, A.C., DeFries, R., Achard, F., Ramankutty, N. and Scholes, R.J. (2005) A synthesis of information on rapid land-cover change for the period1891–2000. *BioScience* 55: 115–124.
60. Liang, J, T. W. Crowther, N. Picard, S. Wiser, M. Zhou, G. Alberti, E.-D. Schulze, A. D. McGuire, F. Bozzato, H. Pretzsch, S. de-Miguel, A. Paquette, B. Herault, M. Scherer-Lorenzen, C. B. Barrett, H. B. Glick, G. M. Hengeveld, G.-J. Nabuurs, S. Pfautsch, H. Viana, A. C. Vibrans, C. Ammer, P. Schall, D. Verbyla, N. Tchebakova, M. Fischer, J. V. Watson, H. Y. H. Chen, X. Lei, M.-J. Schelhaas, H. Lu, D. Gianelle, E. I. Parfenova, C. Salas, E. Lee, B. Lee, H. S. Kim, H. Bruelheide, D. A. Coomes, D. Piotto, T. Sunderland, B. Schmid, S. Gourlet-Fleury, B. Sonke, R. Tavani, J. Zhu, S. Brandl, J. Vayreda, F. Kitahara, E. B. Searle, V. J. Neldner, M. R. Ngugi, C. Baraloto, L. Frizzera, R. Ba azy, J. Oleksyn, T. Zawi a-Nied wiecki, O. Bouriaud, F. Bussotti, L. Finer, B. Jaroszewicz, T. Jucker, F. Valladares, A. M. Jagodzinski, P. L. Peri, C. Gonmadje, W. Marthy, T. OBrien, E. H. Martin, A. R. Marshall, F. Rovero, R. Bitariho, P. A. Niklaus, P. Alvarez-Loayza, N. Chamuya, R. Valencia, F. Mortier, V. Wortel, N. L. Engone-Obiang, L. V. Ferreira, D. E. Odeke, R. M. Vasquez, S. L. Lewis, P. B. Reich. (2016) Positive biodiversity-productivity relationship predominant in global forests**.** *Science* 354: 6309
61. Lillesand, T. M. and Kiefer, R. W. (1999) Remote sensing and image interpretation. New York: John Wiley and Sons.
62. Lo Seen, D., Ramesh, B. R., Nair, K. M.. Martin, M., S. Arrouay, D. and Bourgeon, G. (2010) Soil carbon stocks, deforestation and land-cover changes in the Western Ghats biodiversity hotspot (India). *Global Change Biology* 16: 1777–1792.
63. Lu, D., Batistella, M. and Moran, E. (2004) Multitemporal spectral mixture analysis for Amazonian land-cover change detection. *Canadian Journal of Remote Sensing* 30: 87–100.
64. Lu, D., Mausel, P., Batistella, M. & Moran, E. (2005) Land cover binary change detection methods for use in -the moist tropical region of the Amazon: a comparative study. *International Journal of Remote Sensing* 26: 101-114.

65. Lu,D., Mausel, P., Brondizio, E. and Moran, E. (2001) Assessment of atmospheric correction methods for Landsat TM data applicable to Amazon basin LBA research. *International Journal of Remote Sensing* 23: 2651–2671
66. Malila, W.A. (1980) Change vector analysis: an approach for detecting forest changes with Landsat,in: Proceedings of the 6th Annual Symposium on Machine Processing of Remotely Sensed Data. Purdue University, West Lafayette, IN, pp: 326-335.
67. Mašková, Z., Zemek, F. and Květ, J. (2008) *Normalized difference vegetation index (NDVI) in the management of mountain meadows. Boreal Environment Research* 13: 417–432
68. Matsushita, Bunkei., Yang, Wei., Chen, Jin., Onda, Yuyichi and Qiu, Guoyu. (2007) Sensitivity of the Enhanced Vegetation Index (EVI) and Normalized Difference Vegetation Index (NDVI) to Topographic Effects: A Case Study in High-Density Cypress Forest. *Sensors* 7: 2636–2651.
69. Maxwell, A.E., Strager, M.P., Yuill, C. B. and Petty, J.T. (2012) Modeling Critical Forest Habitat in the Southern Coal Fields of West Virginia. *International Journal of Ecology* 2012: 1–10.
70. McDermid, G.J., Franklin, S.E. and LeDrew, E.F. (2005) Remote sensing for large-area habitat mapping. *Progress in Physical Geography* 29: 449-474.
71. McIver, D. and Wheaton, E. (2005) Tomorrow's forests: adapting to a changing climate. *Springer* pp. 273–282.
72. Menon, S. and Bawa, K.S. (1997) Applications of geographic information systems, remote-sensing, and a landscape ecology approach to biodiversity conservation in the Western Ghats. *Current Science* 73: 134-144.
73. Mir, R.R., Allah, M. Zaman, Sreenivasulu, N., Trethowan, R. and Varshney, R.K. (2012) Integrated genomics, physiology and breeding approaches for improving drought tolerance in crops. *Theoretical and Applied Genetics* 125: 625-645.
74. Mokhtari, A., Mansor, S.B., Mahmud, A.R. and Helmi, Z.M. (2011) Monitoring the impacts of drought on land use/cover: A developed object-based algorithms for NOAA AVHRR time series data. *Journal of Applied Sciences* 11: 3089-3103.
75. Myers, N., Mittermeier, R.A., Mittermeier, C.G., Da Fonseca, G.A.B. and Kent, J. (2000) Biodiversity hotspots for conservation priorities. *Nature 403*: 853-858.
76. Nemani, R.R., Running,W.S. and Pielke,R.A. (1996) Global vegetation cover changes from coarse resolution satellite data. *Journal of Geophysical Research* 101: 7157–7162.
77. Olsson, L., Eklundh, L. and Ard, J. (2005) A recent greening of the Sahel--trends, patterns and potential causes. *Journal of Arid Environments* 63: 556-566.
78. Paruelo, J.M., Burke, I.C. and Lauenroth,W.K. (2001) Land use impact on ecosystem functioning in eastern Colorado, USA. *Global Change Biology* 7: 631–639.
79. Pathak, Suparn. (2014). New Change Detection Techniques to monitor land cover dynamics in mine environment. *The International Archives of the Photogrammetry, Remote Sensing and Spatial Information Sciences* 8.

80. Patra, P. (2011) Remote Sensing and Geographical Information System (GIS) *The Association for Geographical Studies* :1-28
81. Pettorelli, N., Vik ,J.O., Mysterud, A., Gaillard, J.M, Tucker, C.J, and Stenseth, N.C. (2005) Using the satellite-derived NDVI to assess ecological responses to environmental change. *Trends in ecology & evolution* 20: 503-510.
82. Potter, C., Li, S. and Hiatt, C. (2012) Declining Vegetation Growth Rates in the Eastern United States from 2000 to 2010. *Natural Resources* 3: 184-190.
83. Prabhakar, R (1994) Resource, Use, Culture and Ecological Change: A Case Study of the Nilgiri Hills of Southern India. PhD Thesis. CES, *Indian Institute of Science* Bangalore.
84. Rajendran, K., Kitoh, A. and Srinivasan, J. (2012) Monsoon circulation interaction with Western Ghats orography under changing climate. Theoretical and Applied Climatology 110: 555–571.
85. Ramachandra, T. V, & Kumar, U. (2004) Geographic Resources Decision Support System for land use, land cover dynamics analysis, (September), 12–14.
86. Ramaswami, G. and Sukumar, R. (2013) Long-Term Environmental Correlates of Invasion by Lantana camara (Verbenaceae) in a Seasonally Dry Tropical Forest. *PLoS One* 8: e76995.
87. Ramesh, B.R., Menon, S. and Bawa.K.S. (1997) A Vegetation Based Approach to Biodiversity Gap Analysis in the Agastyamalai Region, Western Ghats, India. *Ambio* 26: 529-536.
88. Rasshed, Tarek., Weeks, J.R. and Gadalla, M.S. (2001) Revealing the Anatomy of cities through Specrtal Mixture analysis of multispectral satellite imagery: A case study of the Greater Cario Region, Egypt. *Geocarto International* 16: 5-15.
89. Riiters, K., Wickham, J., Costanza, J. and Vogt, P. (2016) Global Forest Area Trends Underestimate Threats from Forest Fragmentation. *Landscape Ecology*. 31: 137-148.
90. Rindfuss, R.R., Walsh, S.J., Turner, B.L., Fox, J. and Mishra, V. (2008) Developing a science of land change: challenges and methodological issues. *PNAS* 101: 13976–13981.
91. Rocha, A.V. and Shaver, G.R. (2009) Advantages of a two band EVI calculated from solar and photosynthetically active radiation fluxes. *Agricultural and Forest Meteorology* 149: 1560–1563.
92. Rogan, J., Franklin, J. and Roberts, D.A. (2002) A comparison of methods for monitoring multitemporal vegetation change using Thematic Mapper imagery. *Remote Sensing of Environment* 80: 143-156.
93. Roxy, M. K., Ritika, Kapoor., Terray, Pascal., Murtugudde, Raghu., Ashok, Karumuri. and Goswami, B.N. (2015) Drying of Indian subcontinent by rapid Indian Ocean warming and a weakening land-sea thermal gradient. Nature Communication 6: 7423.
94. Running, S. W., Justice, C., Salomonson, V., Hall, D., Barker, J., Kaufman, Y., Strahler, A., Huete, A., Muller, J. P., Vanderbilt, V., Wan, Z. M., Teillet, P. and Carneggie, D.

(1994) Terrestrial remote sensing science and algorithms planned for EOS/MODIS. *International Journal of Remote Sensing* 15: 3587– 3620.

95. Sankar, G. Muthu. (2011) Simple vegetation map of the Western Ghats with 14-classes of vegetation. French Institute Pondicherry.
96. Schmugge, T. J., Kustas, W. P., Ritchie, J. C., Jackson, T. J. and Rango, A. (2002). Remote sensing in hydrology. *Advances in Water Resources* 25: 1367–1385.
97. Schroter, D., et al. (2005) Ecosystem service supply and vulnerability to global change in Europe. *Science* 310: 1333–1337.
98. Setiawan, Y., Yoshino, K. and Philpot, W.D. (2013) Characterizing temporal vegetation dynamics of land use in regional scale of Java Island., Indonesia. Journal of Land Use *Science* 8: 1–30.
99. Shengpei, Dai., Bo. Zhang., Haijun, Wang., Yamin, Wang., Lingxia, Guo., Xingmei, Wang. and Dan, LI. (2011) Vegetation cover change and the driving factors over northwest China. *Journal of Arid Land* 3: 25−33.
100. Singh, A. (1989) Digital change detection techniques using remotely sensed data. *International Journal of Remote Sensing* 10: 989–1003.
101. Smith, Joyotee. and Scherr, S.J. (2003) Capturing the Value of Forest Carbon for Local Livelihoods. *World Development* 31: 2143–2160.
102. Spruce, J.P., Sader, S., Ryan, R.E., Smoot, J., Kuper, P., Ross, K. and Prados, D. (2011) Assessment of MODIS NDVI time series data products for detecting forest defoliation by gypsy moth outbreaks. *Remote Sensing of Environment* 115: 427–437.
103. Sukumar, R. (1990) Nilgiri Biosphere Reserve – From theory to practice. Pages 27-33. In: Proceedings MAB regional training workshop. Tropical forest ecosystems conservation and development in south and south-east Asia. KFRI, Peechi.
104. Sukumar, R., Dattaraja, H.S., Suresh, H.S., Radhakrishnan, J., Vasudeva, R., Nirmala,S., Joshi, N.V. (1992). Long term monitoring of vegetation in a tropical deciduous forest in Mudumalai, southern India. *Current Science* 62: 9.
105. Tucker, C.J. (1979) Red and photographic infrared linear combination for monitoring vegetation. *Remote Sensing of Environment* 8: 127-150.
106. Van der Werf, G.R., Randerson, J.T., Giglio, L., Collatz, G.J., Kasibhatla, P.S. and Arellano Jr, A.F. (2006) Interannual variability in global biomass burning emissions from 1997 to 2004. *Atmospheric Chemistry Physics* 6: 3423–3441.
107. Verbesselt, J., Hyndman, R., Zeileis, A. and Culvenor, D. (2012) Phenological change detection while accounting for abrupt and gradual trends in satellite image time series. *Remote Sensing of Environment* 114: 2970–2980.
108. Vicca, Sara., Balzarolo, Manuela., Filella, Iolanda., Granier, André.,Herbst, Mathias., Knohl, Alexander., Longdoz, Bernard., Mund, Martina., Nagy, Zoltan.,Pintér, Krisztina., Rambal, Serge., Verbesselt, Jan., Verger, Aleixandre., Zeileis, Achim., Zhang, Chao., Peñuelas, Josep. (2016) Remotely-sensed detection of effects of extreme droughts on gross primary production. *Scientific Reports* 6: 28269.

109. Vuolo, Francesco., Richterb, Katja. and Clement, Atzberger. (2011) Evaluation of time-series and phenological indicators for land cover classification based on MODIS data. *Remote Sensing for Agriculture, Ecosystems, and Hydrology XIII* 8174.
110. Waring, R.H., Coops, N.C., Running, S.W. (2011) Predicting Satellite-Derived Patterns of large Scale Disturbances in Forests of the Pacific Northwest Region in response to recent Climatic Variation. *Remote Sensing of Environment* 115: 3554–3566.
111. Westerling, A.L., Hidalgo, H.G., Cayan, D.R. and Swetnam, T.W. (2006) Warming and earlier spring increase western USA wildfire activity. *Science* 313: 940-943.
112. Wilhite, D.A. and Glantz, M.H. (1985) Understanding the drought phenomenon: The role of definitions. Water International 10: 111-120.
113. Wood, S.N. (2006) Generalized additive models: an introduction with R. Chapman and Hall/CRC Press, London.
114. Wulder, M. (1998) Optical remote sensing techniques for the assessment of forest inventory and biophysical parameters. *Progress Physical Geography* 22: 449–476.
115. Wulder, M.A., Franklin, S.E., White, J., Cranny, M., and Dechka, J. (2004) Inclusion of topographic attributes in an unsupervised classification of satellite imagery. *Canadian Journal of Remote Sensing* 30: 137–149.
116. Yadav, P. K., Kapoor, M., and Sarma, K. (2012) Land Use Land Cover Mapping, Change Detection and Conflict Analysis of Nagzira-Navegaon Corridor, Central India Using Geospatial Technology 1: 90–98.
117. Yang, J., Weisberg, J.P. and Bristow, A.N. (2012) Landsat remote sensing approaches for monitoring long-term tree cover dynamics in semi-arid woodlands, Comparison of vegetation indices and spectral mixture analysis. *Remote Sensing of Environment* 119: 62–71.
118. Zhengming, Wan., Pengxin, Wang., and Xiaowen, Li. (2004) Using MODIS Land Surface Temperature and Normalized Difference Vegetation Index Products for Monitoring Drought in the Southern Great Plains, USA. *International Journal of Remote Sensing* 25: 61-72.

Appendix:

1. ASSESSING ABOVEGROUND BIOMASS

The main objective this report was to assess the aboveground biomass changes which is useful for REDD inventories. Sampling was carried out using a 8 km by 8 km grid method where we sampled at least one or two transects (500m x 10m each) depending on the heterogeneity of the area. Global Forest tree cover dataset (http://www.globalforestwatch.org/) was used; it was divided into four classes with % tree cover. Three layer of information, i.e. fuel loads, regeneration and species composition, were obtained from each transect. All individuals ≥30 cm DBH were enumerated along each transect and identified to species following Kodandapani et al (2008). We used allometric equations developed by Centre for Tropical Forest Science (https://cran.r-project.org/src/contrib/Archive/CTFS/) which are based on the categories of forest types, with different equation for moist and dry forest. Seven transects of 500m x 10m each were laid in the field in three vegetation types for biomass estimation.

CTFS Allometric equations for different forest types:

1. Computation for moist forest type

AGB=wsg.vct*exp(RSE[2]+(-1.562)+(2.148*ldbh)+(0.207*ldbh^2)+(0.0281*ldbh^3))

2. Computation for dry forest type

AGB=wsg.vct*exp(RSE[2]+(-0.73)+(1.784*ldbh)+(0.207*ldbh^2)+(-0.0281*ldbh^3))

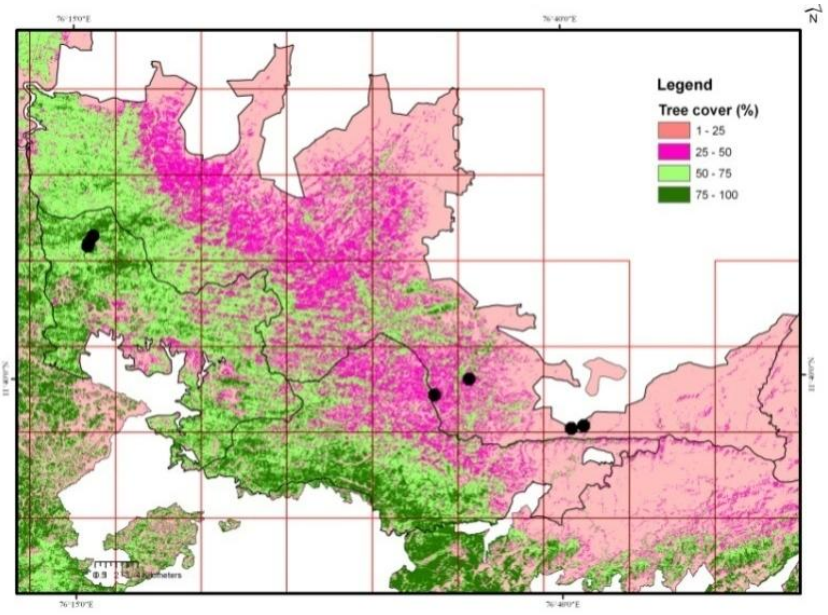

Figure: 1 Transects locations in the study area with tree cover data

Table: 1. Biomass estimates (tons per ha) obtained from each transect.

Transect no.	Vegetation type	Biomass in t/ha	Regeneration Inventory (saplings and seedlings)
1	Moist Deciduous	87.32	319
2	Moist Deciduous	113.65	253
3	Moist Deciduous	106.93	406
4	Dry thorn	39.81	331
5	Dry thorn	71.83	423
6	Dry deciduous	118.0	353
7	Dry deciduous	127.95	605

The highest biomass is found in dry deciduous type followed by moist deciduous and the least is found in dry thorn forest. Regeneration was also high in areas which are found to be greening due to the spread of *Lantana camara*. Thus, it can be concluded that not only the spread of *Lantana camara* (Ramaswami and Sukumar 2013) but also high rate of regeneration in some parts of the drier forest could have increased greenness.

2. VALIDATION OF INCREASING LONG TERM TREND USING FIELD DATA

Linear regression analysis was used to validate the increasing NDVI/EVI trend over a larger landscape using ground truth data of 21 plots in the study area where *Lantana camara* is widespread.

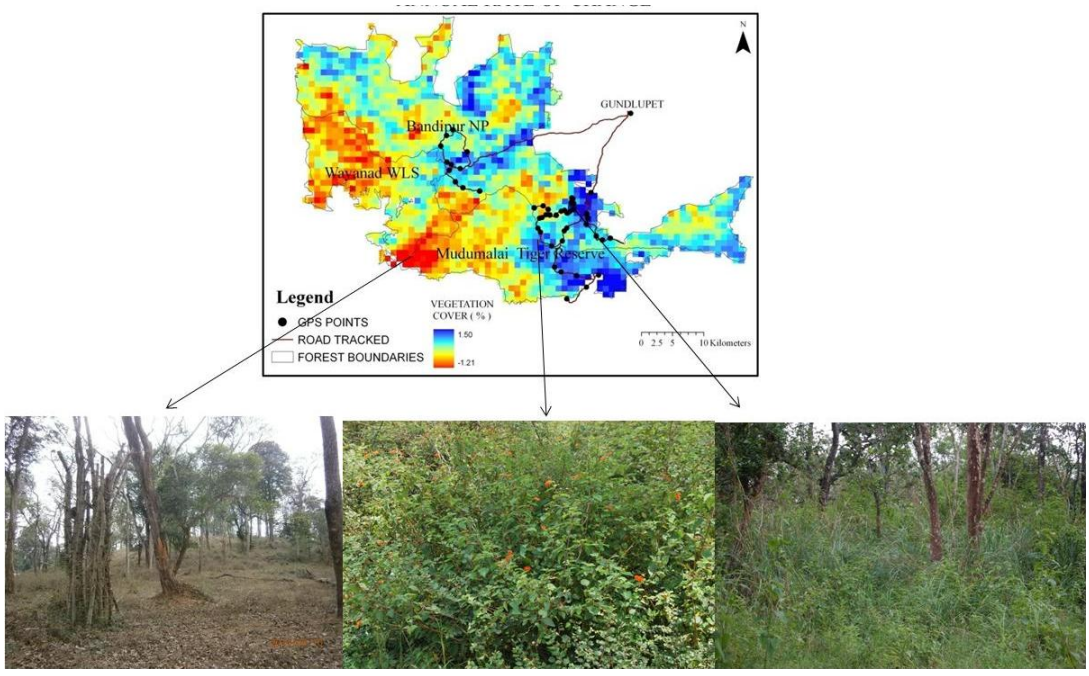

Figure 1: Field validation on the ground

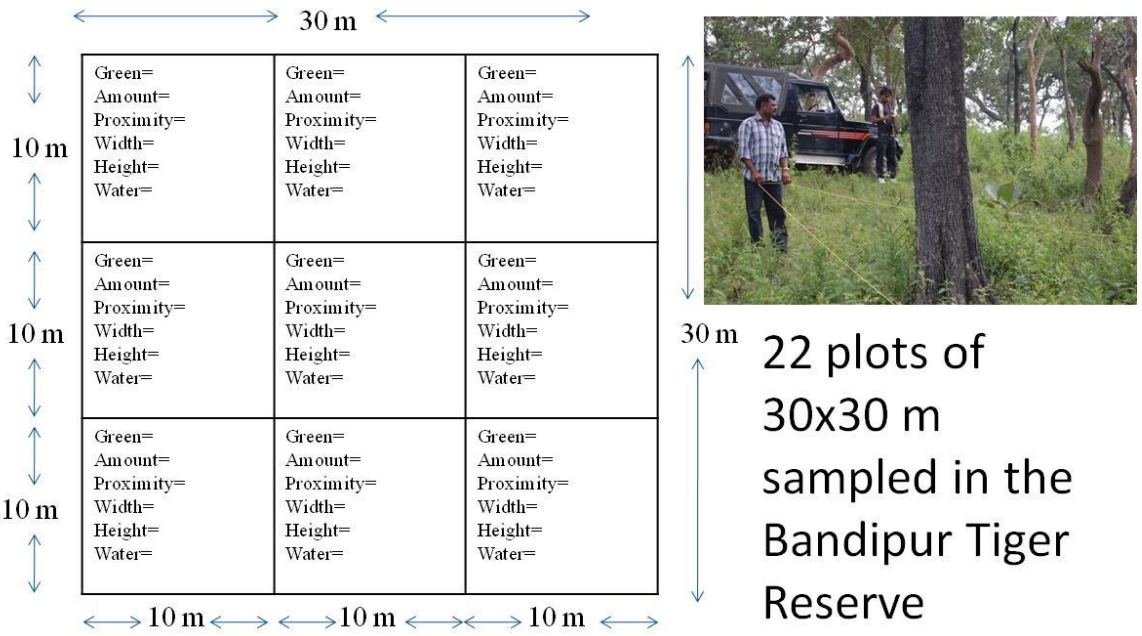

Figure 2: Field sampling methodology.

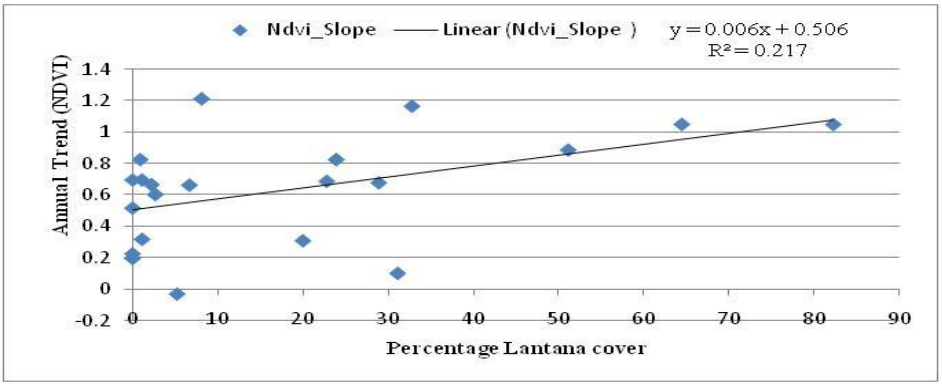

Figure 3: Linear regression for Annual Trend (NDVI) and % of Lantana covered in each plot.

In Bandipur National Park the trend values for NDVI and EVI were extracted from the pixels containing the sample plots. This forest division is mainly covered with dry deciduous forest types. A trend analysis for 21 plots and lantana cover was significant for NDVI trend with 0.033 Adjusted R-squared value, 5.29 F- Statistic and 0.032 P-value, but for the EVI trend it was 0.123 Adjusted R-squared value, 2.669 F- Statistic and 0.118 P-value which was not significant.

3. VALIDATION OF INCREASED GREENING USING IRS SATELLITE DATA

We examined the trends in vegetation in the Sathyamangalam Forest Division using NDVI IRS high resolution time series from 1997 to 2012. A comparison was made of the results between

the coarse and high resolution results of MODIS 10 years' trend analysis and IRS satellite datasets (**Fig 4);** the results were consistent in both datasets. The IRS NDVI trend was classified into six classes, the highest percentage area (36.8%) is found in 0.5-1.0 class while 34.0% of the total area falls in the -0.5 to 0 classes. A similar condition for MODIS classified trend was found where the highest percentage (4.38%) of increasing trend was also found in the 0.5-1.0 class range while was 47.72 % area was in the -0.5 to 0 class. In both the spatial pattern decreasing trends to be around the settlements subject to human disturbance.

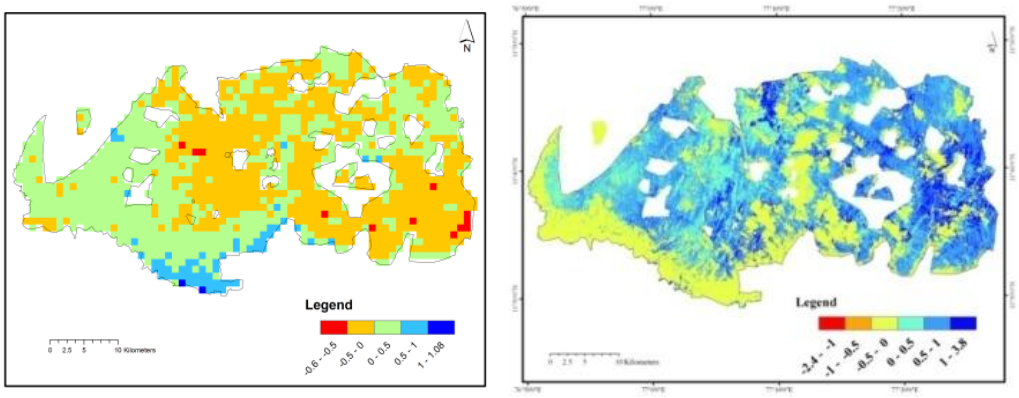

Figure 4: Spatial distribution of slope in the annual trend (ΔNDVI/year-Left) in the study area obtained from MODIS dataset (1 Km Spatial Resolution). Spatial distribution of slope in the annual trend (ΔNDVI/year-Right) in the study area obtained from IRS dataset from 1997 to 2012 NDVI.

4. STANDARD ANOMALY (SA) RESPONSE TO ANNUAL RAINFALL

SA values (NDVI & EVI) were extracted for the Mudumalai 50 hectare plot to examine the response to annual rainfall. There seems to a time lag of about 1 year between rainfall and response of vegetation.

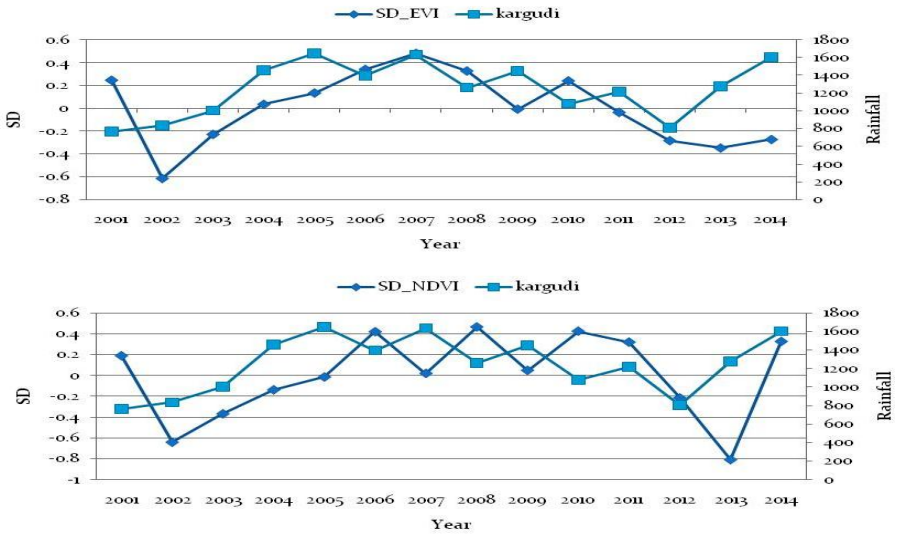

Figure 5: Standard anomaly of 50 hectare plot with ground rainfall station.

5. LAND USE AND LANDCOVER MAP AND PROTECTED AND UNPROTECTED FORESTED DIVISIONS IN THE STUDY AREA.

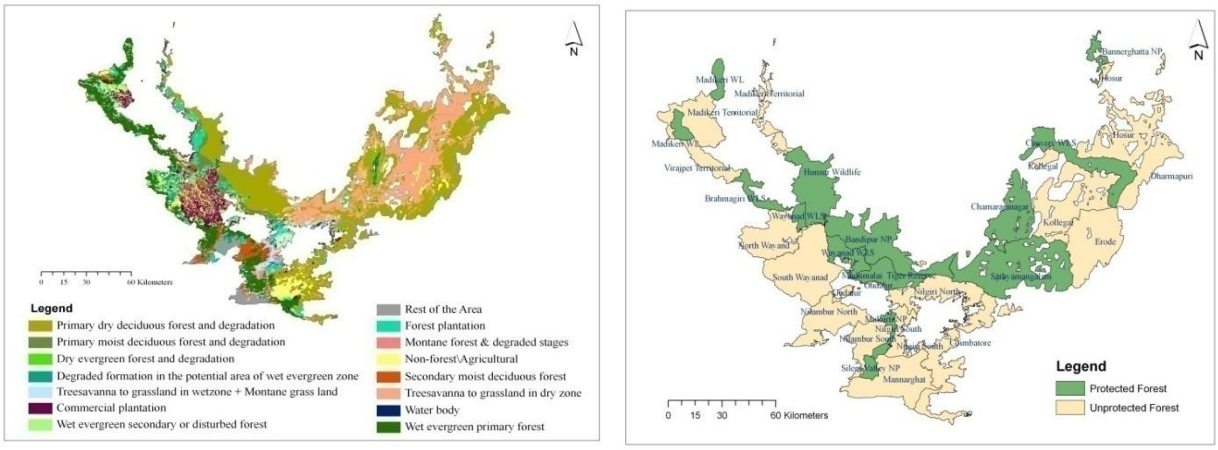

Figure 6: Land use and land cover of the study area (Left) and protected and unprotected forest divisions (Right).

The above (left) figure show the different land use and land cover of the different types of forests from dry deciduous to dry thorn with different legal status of forest. The above right figure shows the forest divisions boundaries in the study area which are divided in to protected and unprotected forest.

6. SPATIAL DISTRIBUTION OF TEMPERATURE AND RAINFALL IN THE STUDY AREA

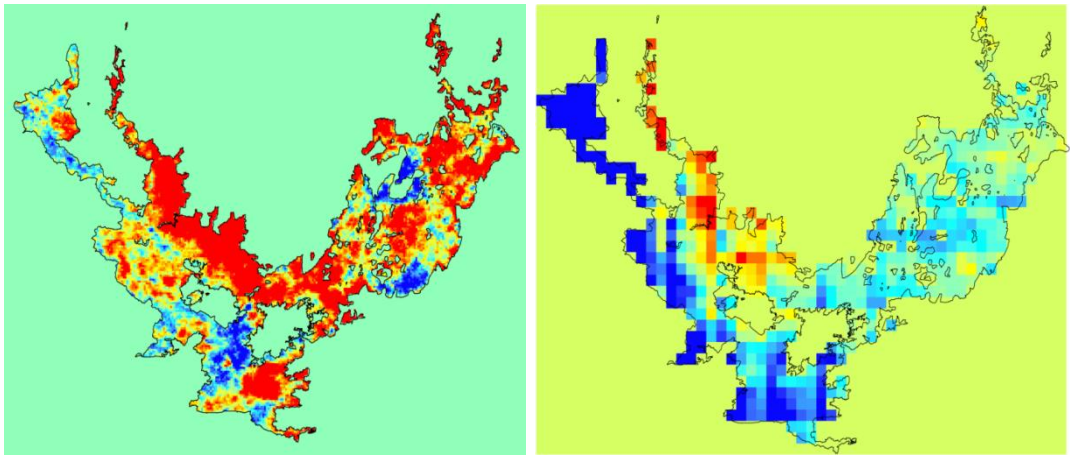

Figure 7: Temperature trend (Left figure) and Rainfall trend (Right).

The above figures show the spatial pattern of trend with red color denotes the decreasing in temperature and rainfall. The blue color denotes the increasing temperature and rainfall over the

study area. The rainfall data is for 30 years with a spatial resolution whereas the temperature is at 5km spatial resolution and where as temperature is for 14 years with 1 km spatial resolution.

7. MAPPING BURNED AREA IN NBR

IRS satellite data were procured from National Remote Sensing Centre, Hyderabad, in digital format for fire mapping for the years 2009, 2012 and 2014.

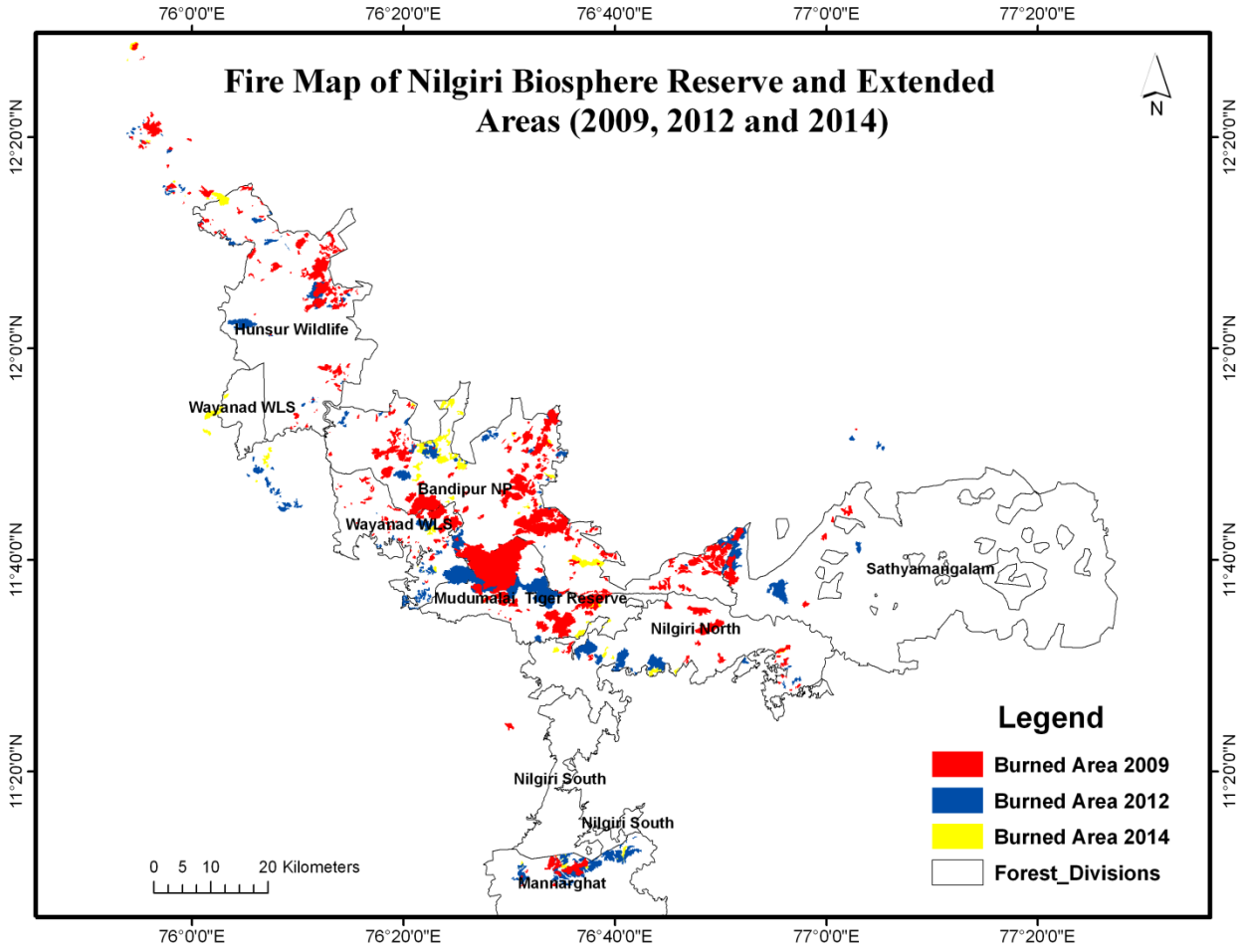

Figure 8: Fire map for the three years- 2009, 2012 and 2014.

In the above figure burned area was mapped for different years using the visual interpretation keys along with False Colour Composite (FCC) to identify the burn scar. A total of 381.7 km^2 area was burned during the year 2009, which could be attributed to failure of northeast or retreating monsoon during the year 2008 or extended dry season in 2009. In 2012 the area reduced to 241.3 km^2which was burned and in 2014 it reduced to 65.8 km^2. The dry regions of the study area with dry deciduous forest, dry thorn forest and scrub was mainly burned.